GASTROENTEROLOGY 2011;140:2000–2008

BASIC—ALIMENTARY TRACT

Loss of Adiponectin Promotes Intestinal Carcinogenesis in *Min* and Wild-type Mice

MICHIHIRO MUTOH,* NAOYA TERAOKA,* SHINJI TAKASU,* MAMI TAKAHASHI,* KUNISHIGE ONUMA,* MASAFUMI YAMAMOTO,* NAOTO KUBOTA,‡ TAKAMOTO ISEKI,‡ TAKASHI KADOWAKI,‡ TAKASHI SUGIMURA,* and KEIJI WAKABAYASHI*,§

*Cancer Prevention Basic Research Project, National Cancer Center Research Institute, Tokyo, Japan; ‡Department of Diabetes and Metabolic Diseases, Graduate School of Medicine, The University of Tokyo, Tokyo, Japan; and §Graduate School of Food and Nutritional Sciences, University of Shizuoka, Shizuoka, Japan

BACKGROUND & AIMS: Metabolic syndrome- and obesity-associated cancers, including colon cancer, are common in Western countries. Visceral fat accumulation and decreased levels of plasma adiponectin (APN) have been associated with development of human colorectal adenoma. We investigated the function of APN in intestinal carcinogenesis. **METHODS:** $APN^{+/+}$, $APN^{+/-}$, or $APN^{-/-}$ mice (C57BL/6J) were given injections of azoxymethane (AOM), which led to development of intestinal tumors; these strains of mice were also crossed with *Min* mice to assess polyp formation. Adipocytokine levels and phosphorylation/activation of AMP-activated protein kinase (AMPK) were evaluated to investigate the mechanisms of APN in tumor growth. **RESULTS:** The total number of polyps in the intestines of male $APN^{+/-}$ *Min* and $APN^{-/-}$*Min* mice increased 2.4- and 3.2-fold, respectively, by the age of 9 weeks and 3.2- and 3.4-fold, respectively, by 12 weeks, compared with those of $APN^{+/+}$*Min* mice. Similar results were obtained from female mice. AOM induced colon tumor formation in 40% of $APN^{+/+}$, 50% of $APN^{+/-}$, and 71% of $APN^{-/-}$ ($P < .05$) mice, respectively; mean values for tumor multiplicity of each genotype were 0.5, 0.6, and 1.1 ($P < .05$), respectively. Phosphorylation of AMPK decreased in intestinal epithelial cells of $APN^{-/-}$ mice compared with $APN^{+/+}$ mice. Among serum adipocytokines, plasminogen activator inhibitor−1 levels increased in $APN^{-/-}$*Min* mice and $APN^{-/-}$ mice that received injections of AOM. Activation of AMPK suppressed expression of plasminogen activator inhibitor−1 in *Min* mice. **CONCLUSIONS: Mice with disruptions in *APN* develop more intestinal tumors and have decreased activation (phosphorylation) of AMPK and increased levels of plasminogen activator inhibitor−1, compared with wild-type mice. APN and its receptor might be developed as targets for cancer chemopreventive agents.**

Keywords: *Apc*-Deficient Mice; Adipokine; Colorectal Cancer; Chemoprevention

The criteria for metabolic syndrome include obesity, hyperlipidemia, type 2 diabetes, and hypertension. Several cancers, including colon cancer, are demonstrated to be associated with metabolic syndrome.[1-5] Obesity-associated cancers are common in Western countries, and they are currently increasing in Eastern countries as well. However, the mechanisms underlying how metabolic syndrome is associated with carcinogenesis remain to be fully understood. Insulin resistance, with hyperinsulinemia, hyperlipidemia, and hyperglycemia, are suggested to be involved in the promotion of colon cancer growth. In addition, dysregulation of adipocytokines, such as adiponectin (APN), leptin, plasminogen activator inhibitor-1 (PAI-1), and tumor necrosis factor−α (TNFα) has been shown to play a crucial role in the pathogenesis of the metabolic syndrome and postulated to promote carcinogenesis.[6] In human clinical studies, it has been reported that the amount of visceral fat positively correlates with colon adenoma risk, and serum APN levels show a negative correlation.[7]

APN is present at high levels in plasma (range, 3−30 μg/mL) as multimers. Both plasma APN and APN messenger RNA (mRNA) in adipose tissue are inversely correlated with body mass index and whole-body adipose mass. Furthermore, a decrease in plasma APN levels is associated with insulin resistance, type 2 diabetes, and coronary artery disease. Physiological functions of APN are elicited through 2 isoforms of its receptor, Adipo-R1 and Adipo-R2, stimulating AMP-activated protein kinase

Abbreviations used in this paper: ACF, aberrant crypt foci; AMPK, AMP-activated protein kinase; AOM, azoxymethane; APN, adiponectin; CK2β, casein kinase 2β; IL-1β, interleukin-1β; MCP-1, monocyte chemotactic protein-1; mRNA, messenger RNA; Pai-1, plasminogen activator inhibitor−1; PCR, polymerase chain reaction; RACK1, receptor for activated protein C kinase 1; TG, triglyceride; TNFα, tumor necrosis factor−α.

0016-5085/$36.00
doi:10.1053/j.gastro.2011.02.019

(AMPK) and peroxisome proliferator–activated receptor-α, respectively.[8]

Recently, we reported an age-dependent hypertriglyceridemic state with low expression levels of hepatic and intestinal lipoprotein lipase mRNA in *Apc*-deficient *Min* and *Apc*1309 mice, animal models of familial adenomatous polyposis.[9,10] Lipoprotein lipase catalyzes the hydrolysis of triglyceride (TG). Moreover, adipocytokines including plasminogen activator inhibitor–1 (Pai-1) were found to be remarkably overexpressed in the livers of *Min* mice as compared to wild-type mice.[11] In addition, hepatic APN mRNA levels were down-regulated in *Min* mice. Administration of Pai-1 blockers, SK-216 or SK-116, demonstrated the involvement of Pai-1 in the production of number of intestinal polyps.

It is assumed that adipocytokines have an impact on carcinogenesis. However, little is known about how their altered regulation is related to the development and progression of colon cancers. Thus, in the present study, we mated APN-deficient C57BL/6J mice with *Min* mice to investigate the effect of genetic inactivation of APN on intestinal carcinogenesis. APN deficiency resulted in increased intestinal polyp development. Moreover, a similar contribution was evident when APN-deficient C57BL/6J mice were treated with azoxymethane (AOM) to induce colon cancer. Reduced phosphorylated(p)-AMPK levels and increased p-Akt levels were suggested to be involved in the accelerated development of intestinal tumors. Moreover, the mechanistic consequences derived from the altered adipicytokines, APN and Pai-1, were demonstrated.

Materials and Methods

Animals

APN-deficient mice (C57BL/6J mice background) were generated as described previously and their genotypes were confirmed by polymerase chain reaction (PCR).[12] Both sexes were used at 6 weeks of age. Female C57BL/6-*Apc*$^{Min/+}$ mice (*Min* mice), 5 weeks of age, were purchased from The Jackson Laboratory (Bar Harbor, ME) and genotyped by the method reported previously. Heterozygotes of the female *Min* mice were mated with *APN*$^{-/-}$ C57BL/6J males to generate *APN*$^{+/-}$*Min* mice. Such males were crossed again with *APN*$^{+/-}$ C57BL/6J females to give *APN*$^{-/-}$*Min* mice. Offspring were genotyped by PCR.[9] In all the animal experiments in the present study, a maximum of 5 animals were housed per plastic cage, with sterilized softwood chips as bedding, in a barrier-sustained animal room, air-conditioned at 24 ± 2°C and 55% humidity, on a 12-hour light-to-dark cycle. AIN-76A powdered basal diet (CLEA Japan, Tokyo, Japan) and water were available ad libitum. The animals were observed daily for clinical signs and morbidity, and body weights and food consumption were measured weekly. At the sacrifice time point, mice were anesthetized with ether, and blood samples were collected from the abdominal vein. The experiments were conducted according to the Guidelines for Animal Experiments in the National Cancer Center and were approved by the Institutional Ethics Review Committee for Animal Experimentation in the National Cancer Center.

Experimental Protocol for APN-Deficient Min *and C57BL/6JMice*

Both sexes of *Min* mice (n = 7) with *APN*$^{+/+}$, *APN*$^{+/-}$, and *APN*$^{-/-}$ genotypes or C57BL/6J mice (n = 4) with *APN*$^{+/+}$, *APN*$^{+/-}$, and *APN*$^{-/-}$ genotypes were used for examination at the ages of 9 and 12 weeks. The levels of serum TG and total cholesterol were measured as reported previously.[10] The liver, kidneys, heart, and spleen were weighed and tissue samples from the liver and intestine were rapidly deep-frozen in liquid nitrogen and stored at −80°C.

The stomach and intestinal tract were removed, filled with 10% buffered formalin, and separated into the stomach, small intestine, cecum, and colon. The small intestine was divided into the proximal segment (4 cm in length), and proximal (middle) and distal halves of the remainder. All segments were opened longitudinally and fixed flat between filter paper in 10% buffered formalin. The numbers and sizes of polyps, and their distributions in the intestine were assessed with a stereoscopic microscope. Slices of the liver, kidneys, heart, and spleen were embedded in paraffin, sectioned, and stained with H&E.

Experimental Protocol for APN$^{+/-}$Min *Mice With APN Treatment*

Recombinant full-length murine APN was produced and purified as described previously[13,14] and dissolved in saline at a concentration of 300 μg/mL for use. *APN*$^{+/-}$*Min* mice of both sexes were divided into an APN-injected group (n = 10 each) and saline-injected control group (n = 10 each). Their body weight was measured and 1.5 mg/kg APN or the same volume of saline was intraperitoneally injected once a week from the age of 6 weeks to 12 weeks (6 times) following the method used in the previous report.[15] The numbers and sizes of polyps, and their distributions in the intestine were examined.

AOM-Induced Colon Tumor Development in APN-Deficient C57BL/6J Mice

Six-week-old male *APN*$^{+/+}$, *APN*$^{+/-}$, and *APN*$^{-/-}$ C57BL/6J mice (n = 30 each) received AOM at a dose of 10 mg/kg body weight intraperitoneally once a week for 6 weeks. Male *APN*$^{+/+}$ and *APN*$^{-/-}$ C57BL/6J mice (n = 10 each) without AOM treatment were used for evaluating sporadic colorectal cancer development. After laparotomy at 55 weeks of age, the entire intestines were resected and opened longitudinally and the contents

were flushed with normal saline. Using a dissection microscope, colon tumors were noted grossly for their location, number, and diameter, and measured with calipers. All tumors from AOM-treated C57BL/6J mice were subjected to histological examination after routine processing and H&E staining. The remaining small intestinal mucosa was removed by scraping and used for AMPK measurement. High-density lipoprotein cholesterol was assessed by FUJI DRI-CHEM4000 (FUJIFILM Medical Co., Ltd., Tokyo, Japan). Total body fat amount was determined by EchoMRI-100 (Echo Medical Systems, Houston, TX).

AOM-Induced Colon Aberrant Crypt Foci Development in APN-Deficient Mice Treated With Pai-1 Blocker

Male $APN^{-/-}$ C57BL/6J mice (n = 10 each) of 6 weeks in age received AOM at a dose of 10 mg/kg body weight intraperitoneally once a week for 3 weeks. From the first treatment with AOM, mice were fed control AIN-76A or experimental diet containing Pai-1 blocker SK-216,[11] chemically synthesized at Shizuoka Coffein Co. Ltd., at 50 and 100 ppm for 8 weeks. All mice were sacrificed 5 weeks after the first dose of AOM. After laparotomy, the entire colons were resected, fixed, stained with 0.2% methylene blue and scored for the number of aberrant crypt foci (ACF)/colon according to the procedure of previous report.[16]

Experimental Protocol for Min *Mice Treated With Metformin*

To investigate the effects of AMPK activation on Pai-1 expression levels, four male *Min* mice at 6 weeks of age were given 1000 ppm metformin, 1,1-dimethylbiguanide hydrochloride (Wako Chemical, Osaka, Japan) in the diet for 14 weeks and liver samples were collected. Control group mice were fed basal diet without metformin.

Detection of Intestinal Phosphorylated AMPK Levels

The concentrations of p-AMPK in the small intestine (n = 4) and colon (n = 4) from 9-week-old male $APN^{+/+}$, $APN^{+/-}$, and $APN^{-/-}$ C57BL/6J mice, and in the liver (n = 4) from 12-week-old male $APN^{+/+}$ *Min*, $APN^{+/-}$ *Min*, and $APN^{-/-}$*Min* mice were determined using an AMPKα [pT172] enzyme-linked immunosorbent assay kit (Invitrogen, Carlsbad, CA), according to the manufacturer's protocol. Concentrations of p-Akt and total Akt in the small intestine were determined using a PathScan Cell Growth 4-Plex Array Kit (Cell Signaling Technology, Inc., Danvers, MA) for 6 samples from 55-week-old male $APN^{+/+}$, $APN^{+/-}$, and $APN^{-/-}$ C57BL/6J mice, according to the manufacturer's protocol.

Real-Time PCR Analysis and Reverse Transcription PCR Analysis

Tissue samples from livers of male *Min* mice with $APN^{+/+}$, $APN^{+/-}$, and $APN^{-/-}$ genotypes and C57BL/6J mice with $APN^{+/+}$, $APN^{+/-}$, and $APN^{-/-}$ genotypes were used. Total RNA was isolated from tissues using Isogen (Nippon Gene, Tokyo, Japan), treated with DNase I (Invitrogen) and 3 μg aliquots in a final volume of 20 μL were used for synthesis of complementary DNA using an Omniscript RT Kit (Qiagen, Hilden, Germany) and an oligo(dT) primer. Primers for mouse Adipo-R1, mouse Adipo-R2, and glyceraldehyde-3-phosphate dehydrogenase were employed as reported previously.[17] Cycling conditions were as follows: 94°C for 5 seconds, annealing temperature (60–66°C) for 30 seconds, 72°C for 60 seconds, and 32 cycles after an initial step of 95°C for 3 minutes. A final elongation step of 72°C for 10 minutes completed the PCR. The products were then electrophoresed on 2% agarose gels. Real-time PCR was carried out using a DNA Engine Opticon TM 2 (MJ Japan Ltd., Tokyo, Japan) with SYBR Green Real-time PCR Master Mix (Toyobo Co., Osaka, Japan) according to the manufacturer's instructions. Primers for mouse Pai-1, mouse casein kinase 2β (CK2β), and glyceraldehyde-3-phosphate dehydrogenase were employed as reported previously.[18,19] To assess the specificity of each primer set, amplicons generated from the PCR reaction were analyzed for melting curves and also by electrophoresis in 2% agarose gels.

Determination of Serum Adipocytokine Levels

The concentrations of APN in the plasma were determined using a Quantikine Adiponectin/Acrp30 Immunoassay Kit (R&D Systems, Inc., Minneapolis, MN). Total of 4 or 5 samples from 12-week-old male *Min* mice with $APN^{+/+}$, $APN^{+/-}$, and $APN^{-/-}$ genotypes and 10 samples from 55-week-old C57BL/6J mice with $APN^{+/+}$, $APN^{+/-}$, and $APN^{-/-}$ genotypes, were treated according to manufacturer's protocol. Pai-1, leptin, resistin, TNFα, interleukin (IL)-6, and monocyte chemotactic protein-1 (MCP-1) were measured using Multiplex kits (LINCOplex, St Louis, MO).

Primary Cultures of APN*-Deficient Fibroblast Cells and Treatment With Insulin or IL-6*

Primary cultures of fibroblasts were prepared from newborn $APN^{-/-}$ and $APN^{+/+}$ C57BL/6J mouse epidermis after separation from the dermis by a trypsin flotation method.[20] Cells were maintained in Dulbecco's modified Eagle's medium supplemented with 10% heat-inactivated fetal bovine serum (Hyclone Laboratories, Inc., Logan, UT) at 37°C in 5% CO_2. Fibroblasts were plated in 24-well cell culture dishes at a density of 100,000 cells/dish, with Dulbecco's modified Eagle's medium containing 10% fetal bovine serum. After 12 hours

culture without FBS, 1 μg/mL insulin (Invitrogen) or 50 ng/mL IL-6 (R&D Systems) was added in the medium for 5 or 10 minutes. After treatment, the fibroblasts were lysed in 100 μL lysis buffer (0.0625 M Tris-HCl [pH 6.8], 20% 2-mercaptoethanol, 10% glycerol, 5% sodium dodecyl sulfate) with Halt phosphatase inhibitor cocktail (Pierce Biotechnology, Rockford, IL) and Complete Mini, protease inhibitor cocktail tablets (Roche Diagnostics, Mannheim, Germany). Samples were separated in 10% polyacrylamide gel electrophoresis-sodium dodecyl sulfate gels and transferred onto polyvinylidene difluoride membranes (Millipore, Billerica, MA). Antibodies against the p-Akt (Ser473), p-Erk1/2 (Thr202/Thy204; Cell Signaling Technology), and β-actin (Biomedical Technologies Inc, Stoughton, MA) were used at a 2000× dilution. Antibodies against the Bcl-2 (Santa Cruz Biotechnology, CA) were used at a 200× dilution. Peroxidase-conjugated secondary antibodies for anti-rabbit IgG were obtained from GE Healthcare, Buckinghamshire, UK. Blots were developed with enhanced chemoluminescence (ECL) (GE Healthcare). Protein levels were evaluated by detecting the density of the band using NIH Image 1.62, and the data normalized by the density of β-actin.

Immunohistochemical Staining

Colon with tumors from 55-week-old male C57BL/6J mice of $APN^{+/+}$, $APN^{+/-}$, and $APN^{-/-}$ genotypes (n = 6 each) and the middle segments of the small intestines of 9-week-old male *Min* mice of $APN^{+/+}$, $APN^{+/-}$, and $APN^{-/-}$ genotypes (n = 6 each) were prepared for immunohistochemical examination using polyclonal rabbit anti-receptor for activated protein C kinase 1 (RACK1) antibody (Santa Cruz Biotechnology) and monoclonal mouse anti-CK2β antibody (Pierce Biotechnology) at 100× dilution. As the secondary antibody, biotinylated anti-rabbit IgG and anti-mouse IgG (Vector Laboratories, Burlingame, CA) were employed at a 200× dilution. Staining was performed using avidin-biotin reagents (Vectastain ABC reagents; Vector Laboratories), 3,3′-diaminobenzidine, hydrogen peroxide, and hematoxylin. As a negative control, consecutive sections were immunostained without exposure to the primary antibody.

Statistical Analysis

The significance of differences in the incidences of AOM-induced mouse tumors was analyzed using the χ^2 test and other statistical analyses were performed with the Dunnett's multiple comparison test. Statistical significance was concluded with P values $<.05$.

Results

Generation of APN-Deficient Min *Mice*

To determine the effect of the deficiency of APN on intestinal polyp formation in *Min* mice, we introduced a knockout mutation of the *APN* gene into the *Min* mice by successive cross-mating and generated *Min* mice that carried $APN^{+/-}$ and $APN^{-/-}$ mutations. The quantity of serum APN observed in $APN^{+/+}$*Min* mice, 5.6 μg/mL, was decreased by almost half in $APN^{+/-}$*Min* mice, 3.0 μg/mL, and none was detected in $APN^{-/-}$*Min* mice (Figure 1*A*). APN receptors, Adio-R1 and -R2, were clearly observed, and both expression levels were not affected by APN deficiency (Figure 1*B*). Genotyping did not significantly affect food intake, behavior, or body weight changes during the experimental periods. Final body weights in the 12-week-old male $APN^{+/+}$*Min*, $APN^{+/-}$*Min*, and $APN^{-/-}$*Min* mice were 25.5 ± 1.6, 24.9 ± 1.3 and 23.8 ± 3.0 g, respectively, and in female mice were 20.6 ± 1.7, 20.5 ± 1.5, and 20.1 ± 0.6 g.

An age-dependent change of serum TG levels was observed in $APN^{+/+}$*Min* mice fed basal diet at 9 and 12 weeks of age, the levels rising from 53 to 143 mg/dL in males (Supplementary Figure). Comparing serum levels of TG in APN-deficient male *Min* mice with male

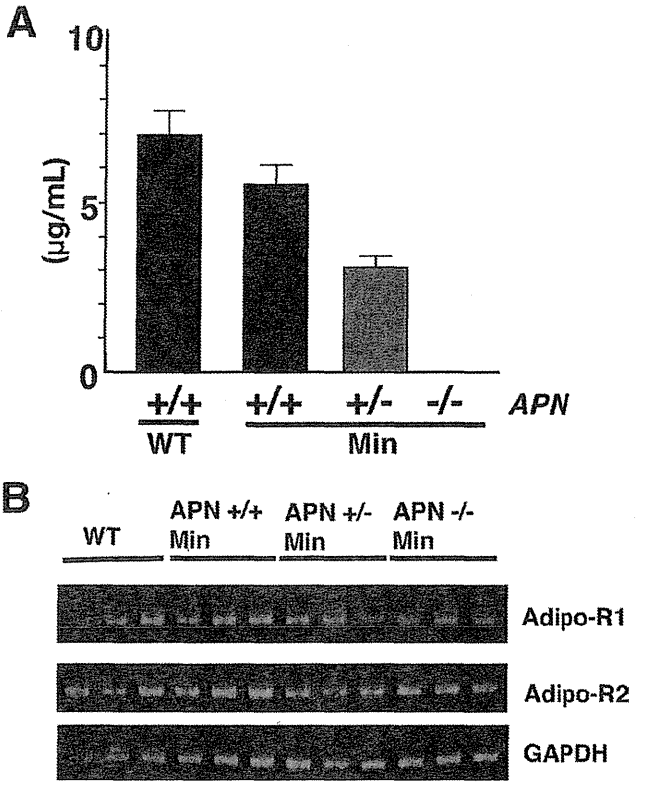

Figure 1. Serum adiponectin (APN) levels and expression levels of APN receptors in *APN*-deficient *Min* mice. (*A*) Serum APN levels for 12-week-old male $APN^{+/+}$*Min*, $APN^{+/-}$*Min*, and $APN^{-/-}$*Min* mice (n = 3) and for 12-week-old male $APN^{+/+}$ mice (n = 4) were evaluated by enzyme-linked immunosorbent assay. (*B*) Liver samples from 12-week-old male *APN*-deficient *Min* mice (n = 3) and for 12-week-old male $APN^{+/+}$ C57BL/6J mice (n = 3) were analyzed for APN receptors, Adipo-R1 and -R2 by reverse transcription polymerase chain reaction analysis. Glyceraldehyde-3-phosphate dehydrogenase was employed as an internal control. WT, wild-type mice.

Table 1. Number of Intestinal Polyps in Male Adiponectin-Deficient *Min* Mice

		No. of polyps/mouse				
		Small intestine				
Age (*wk*)	APN genotype	Proximal	Middle	Distal	Colon	Total
9	+/+	2.1 ± 0.6	8.4 ± 2.7	29.6 ± 11.5	0.1 ± 0.1	40.4 ± 14.5
	+/−	3.6 ± 0.8	23.6 ± 3.4[a]	68.6 ± 9.9[b]	0.7 ± 0.3	96.4 ± 12.3[b]
	−/−	4.0 ± 0.6[b]	26.4 ± 2.3[a]	97.9 ± 12.4[a]	1.1 ± 0.3[b]	128.0 ± 14.2[a]
12	+/+	4.4 ± 1.3	17.1 ± 3.9	52.9 ± 8.8	1.3 ± 0.5	75.7 ± 13.5
	+/−	5.7 ± 1.0	41.5 ± 5.5[a]	130.7 ± 6.6[a]	1.7 ± 0.6	179.2 ± 10.8[a]
	−/−	8.1 ± 1.4	34.7 ± 4.2[b]	111.7 ± 11.2[a]	2.0 ± 0.5	156.6 ± 15.3[a]

NOTE. Data are mean ± standard error (n = 7).
APN, adiponection.
[a]$P < .01$ vs *APN*$^{+/+}$*Min*.
[b]$P < .05$ vs *APN*$^{+/+}$*Min*.

APN$^{+/+}$*Min* mice, a tendency for increase was observed at 9 and 12 weeks of age. Serum levels of total cholesterol were not largely altered with the age and genotypes (Supplementary Figure 1). Similar results regarding serum TG and cholesterol were obtained in female *APN*-deficient *Min* mice.

Intestinal Polyp Formation by APN Knockout Mutation in Min *Mice*

Table 1 shows data for the number and distribution of intestinal polyps in the male *APN*$^{+/+}$*Min*, *APN*$^{+/-}$*Min* and *APN*$^{-/-}$*Min* mice at the 9 and 12 weeks, while data for female mice are given in Supplementary Table 1. The polyps developing in each genotype were all histopathologically identified as adenomas. Development of intestinal polyps in the male *APN*$^{+/-}$*Min* and *APN*$^{-/-}$*Min* mice at 9 weeks were 239% and 317% of the total value in male *APN*$^{+/+}$*Min* mice, respectively, and 319% and 338% of total value in female *APN*$^{+/+}$*Min* mice. At 12 weeks, male *APN*$^{+/-}$*Min* and *APN*$^{-/-}$*Min* mice developed polyps at 237% and 207% of the total value in male *APN*$^{+/+}$*Min* mice, respectively, and 230% and 206% of those in female mice. Representative photographs of the intestinal polyps observed in the male *APN*$^{+/+}$*Min*, *APN*$^{+/-}$*Min*, and *APN*$^{-/-}$*Min* mice at 12 weeks are shown in Supplementary Figure 2.

To confirm the effects of APN on intestinal polyp formation, APN was intraperitoneally injected to *APN*$^{+/-}$*Min* mice. The total number of intestinal polyps was significantly less in the APN-injected group than in saline-injected group in both sexes, as shown in Supplementary Table 2 and Supplementary Figure 2.

Change of Serum Levels of Adipocytokines in APN-Deficient Min *Mice*

In an attempt to clarify mechanisms affecting development of intestinal polyps, we analyzed serum levels for other adipocytokines, including Pai-1, leptin, resistin, TNFα, IL-6, and MCP-1. Among the adipocytokines, Pai-1 levels were significantly increased 1.5-fold and 2.1-fold ($P < .05$) in 12-week-old male *APN*$^{+/-}$*Min* and *APN*$^{-/-}$*Min* mice as compared with *APN*$^{+/+}$*Min* mice, respectively (Table 2), and were also increased in 9-week-old male *APN*$^{+/-}$*Min* and *APN*$^{-/-}$*Min* mice. Serum leptin levels were slightly decreased with APN deficiency. Resistin, TNFα, IL-6, and MCP-1 levels did not appear to depend on the genotypes.

Table 2. Serum Adipocytokine Concentrations in Male Adiponectin-Deficient *Min* Mice

Age (*wk*)	APN genotype	Pai-1, *pg/mL*	Leptin, *pg/mL*	Resistin, *pg/mL*	TNFα, *pg/mL*	IL-6, *pg/mL*	MCP-1, *pg/mL*
9	+/+	1319 ± 108	3632 ± 859	1450 ± 121	5.0 ± 0.4	15 ± 5	35 ± 5
	+/−	1819 ± 117[a]	3163 ± 544	1281 ± 92	5.0 ± 0.3	12 ± 6	32 ± 5
	−/−	1738 ± 105[a]	3196 ± 783	1299 ± 110	5.1 ± 0.3	32 ± 11	34 ± 5
12	+/+	5131 ± 2540	3210 ± 938	989 ± 72	4.7 ± 0.2	20 ± 7	22 ± 6
	+/−	7451 ± 1425	2014 ± 253	1189 ± 133	5.7 ± 0.5	27 ± 6	13 ± 1
	−/−	10693 ± 4542[b]	1792 ± 562	1152 ± 562	6.0 ± 0.6	23 ± 12	19 ± 1

NOTE. Data are mean ± standard error (n = 4–5).
APN, adiponectin; IL-6, interleukin-6; MCP-1, monocyte chemotactic protein-1; Pai-1, plasminogen activator inhibitor−1; TNFα, tumor necrosis factor−α.
[a]$P < .05$ vs 9-week-old *APN*$^{+/+}$*Min*.
[b]$P < .05$ vs 12-week-old *APN*$^{+/+}$*Min*.

Table 3. Incidence and Multiplicity of Azoxymethane-Induced Colon Tumor in Male Adiponectin-Deficient Mice

	Adenoma		Adenocarcinoma		Total	
APN genotype	Incidence (%)	Multiplicity[a]	Incidence (%)	Multiplicity[a]	Incidence (%)	Multiplicity[a]
+/+	4/25 (16)	0.2 ± 0.5	7/25 (28)	0.3 ± 0.6	10/25 (40)	0.5 ± 0.7
+/−	6/28 (21)	0.2 ± 0.4	9/28 (32)	0.4 ± 0.6	14/28 (50)	0.6 ± 0.7
−/−	8/24 (33)	0.3 ± 0.5	12/24 (50)	0.8 ± 1.0	17/24 (71)[b]	1.1 ± 1.0[b]

APN, adiponectin.
[a]Data are mean ± standard deviation.
[b]$P < .05$ vs $APN^{+/+}$.

Colon Tumor Development in APN-Deficient C57BL/6J Mice With AOM Treatment

Male $APN^{+/+}$, $APN^{+/-}$, and $APN^{-/-}$ C57BL/6J mice were treated with AOM. The change of each genotype did not affect food intake, clinical signs, or body weight changes during the experimental period. At the end of the experiment, whole body fat ratios for C57BL/6J mice in each genotype with AOM treatment were almost the same (Supplementary Figure 3), and all genotypes demonstrated similar levels of serum TG, total cholesterol, high-density lipoprotein, and free fatty acids (Supplementary Figure 3).

Data for the incidence and multiplicity of colon tumors are summarized in Table 3. No lesions were apparent without the carcinogen. Total tumor incidences were increased to 50% and 71% ($P < .05$) in $APN^{+/-}$ and $APN^{-/-}$ C57BL/6J mice, respectively, as compared with 40% in wild-type mice. Regarding tumor multiplicity, values were 0.5, 0.6, and 1.1 ($P < .05$) for $APN^{+/+}$, $APN^{+/-}$, and $APN^{-/-}$ C57BL/6J mice, respectively. Histopathological examination revealed that incidence of adenoma in wild-type mice was 16% and adenocarcinoma was 28%, and each incidence tended to be increased with APN deficiency. Moreover, multiplicity of adenocarcinoma tended to be increased with APN deficiency. Average colon tumor diameters for $APN^{+/+}$, $APN^{+/-}$, and $APN^{-/-}$ C57BL/6J mice were 2.8 ± 1.5 (mean ± standard deviation), 3.0 ± 0.9 and 3.4 ± 1.6 mm, respectively.

Change of Adipocytokine Levels by APN Gene Deficiency

We also analyzed serum levels for adipocytokines in 55-week-old male APN-deficient C57BL/6J mice treated with AOM. Among the adipocytokines, Pai-1 levels increased 1.6-fold and 1.7-fold in $APN^{+/-}$ and $APN^{-/-}$ C57BL/6J mice as compared to those in $APN^{+/+}$ C57BL/6J mice, respectively (Table 4). Pai-1 is expressed ubiquitously. Thus, representative Pai-1 expression levels were analyzed using liver samples. Hepatic Pai-1 mRNA levels for 55-week-old male $APN^{+/-}$ and $APN^{-/-}$ C57BL/6J mice increased 1.8-fold and 1.4-fold compared to those in $APN^{+/+}$ mice, respectively. Serum TNFα and MCP-1 levels were slightly decreased in $APN^{+/-}$ and $APN^{-/-}$ C57BL/6J mice compared to those in wild-type mice. Leptin, resistin, and IL-6 levels did not depend on the genotypes.

Analysis of AMPK Activity

To investigate whether AMPK is involved in the regulation of Pai-1, *Min* mice were fed an AMPK activator, metformin, for 14 weeks. Hepatic mRNA levels for Pai-1 in metformin-treated *Min* mice decreased to 28% ($P < .05$) of those in untreated *Min* mice.

To confirm the known molecular signaling from Adipo-R1 that affects the development of intestinal tumors, we analyzed p-AMPK levels in small intestinal epithelial cells. In 9-week-old male $APN^{+/-}$ and $APN^{-/-}$ C57BL/6J mice they were reduced to 53% and 37% of those in $APN^{+/+}$ C57BL/6J mice, respectively (Figure 2*A*). P-AMPK levels in colon epithelial cells also tended to be reduced with APN deficiency (Figure 2*B*). P-AMPK levels in the liver were slightly reduced in APN-deficient *Min* mice (Figure 2*C*). Furthermore, p-Akt levels in intestinal epithelial cells were elevated in $APN^{-/-}$ C57BL/6J mice (Figure 2*D*).

To confirm the existence of AdipoR-binding proteins, RACK1 and CK2β, which regulate proximal signal transduction events in response to APN, immuno-

Table 4. Serum Adipocytokine Concentrations in Azoxymethane-Treated Male Adiponectin-Deficient Mice

APN genotype	Pai-1, *pg/mL*	Leptin, *pg/mL*	Resistin, *pg/mL*	TNFα, *pg/mL*	IL-6, *pg/mL*	MCP-1, *pg/mL*
+/+	1998 ± 249	4612 ± 576	4015 ± 322	44 ± 10	65 ± 12	114 ± 16
+/−	3220 ± 293[a]	3693 ± 558	3554 ± 366	36 ± 4	71 ± 23	103 ± 15
−/−	3470 ± 776	4326 ± 850	4742 ± 274	36 ± 5	69 ± 12	85 ± 12

NOTE. Data are mean ± standard error (n = 10).
APN, adiponectin; IL-6, interleukin-6; MCP-1, monocyte chemotactic protein-1; Pai-1, plasminogen activator inhibitor−1; TNFα, tumor necrosis factor−α.
[a]$P < .01$ vs $APN^{+/+}$.

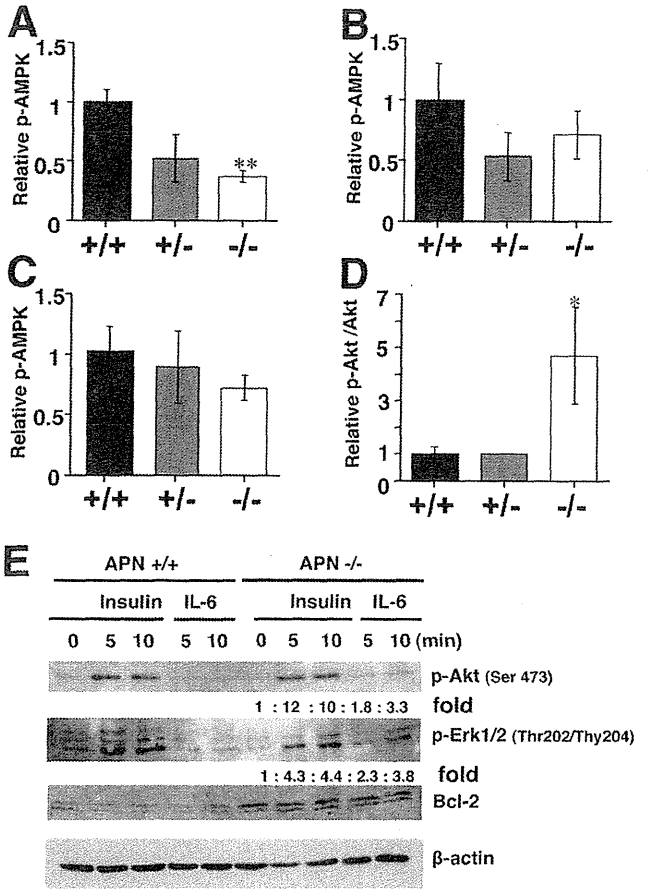

Figure 2. Phosphorylated–AMP-activated protein kinase (p-AMPK) and -Akt levels in adiponectin (*APN*)-deficient mice and its derived fibroblasts. Relative p-AMPK levels in the small intestine (*A*) and colon (*B*) of 9-week-old male $APN^{+/+}$, $APN^{+/-}$, and $APN^{-/-}$ C57BL/6J mice without azoxymethane treatment (n = 4 each), respectively, were evaluated by enzyme-linked immunosorbent assay (ELISA). (*C*) Relative p-AMPK levels in the liver of 12-week-old male $APN^{+/+}$*Min*, $APN^{+/-}$*Min*, and $APN^{-/-}$*Min* mice (n = 4 each) were evaluated by ELISA. (*D*) Relative p-Akt/total Akt levels in the small intestine of AOM-treated 55-week-old male $APN^{+/+}$, $APN^{+/-}$, and $APN^{-/-}$ C57BL/6J mice (n = 6 each) were evaluated by ELISA. *Black*, $APN^{+/+}$; *gray*, $APN^{+/-}$; *white*, $APN^{-/-}$. Data are mean ± standard error. $^{**}P < .01$. $^{*}P < .05$. (*E*) Effects of insulin (1 μg/mL for 5 and 10 minutes treatment) and interleukin-6 (IL-6; 50 ng/mL for 5 and 10 minutes) on the protein expression of p-Akt and -Erk, and Bcl-2 in fibroblasts derived from $APN^{+/+}$ and $APN^{-/-}$ C57BL/6J mice are shown. β-actin was a loading control. Density of the bands was evaluated by NIH image, and the relative level was further normalized by β-actin.

histochemical analysis was performed on the colon tumors of 55-week-old male $APN^{+/+}$, $APN^{+/-}$, and $APN^{-/-}$ C57BL/6J mice treated with AOM and small intestinal polyps of 9-week-old male $APN^{+/+}$*Min*, $APN^{+/-}$*Min*, and $APN^{-/-}$*Min* mice. RACK1 and CK2β were expressed in the epithelial cells of normal colon mucosa and colon tumor at the almost same levels in each genotype (Supplementary Figures 4 and 5). Real-time PCR revealed that the expression levels of CK2β were almost the same among the colon mucosa of 9-week-old male $APN^{+/+}$, $APN^{+/-}$, and $APN^{-/-}$ C57BL/6J mice (data not shown). The expression levels of RACK1 and CK2β were weakly observed in the nontumorous parts and intestinal polyps of *Min* mice, and expressions were at almost the same levels in each genotype (Supplementary Figures 4 and 5).

Effects of Pai-1 Blocker on Colon ACF Development in $APN^{-/-}$ C57BL/6J Mice With AOM Treatment

To clarify if Pai-1 might be involved in colon carcinogenesis, we used a short-term in vivo model using ACF formation induced by AOM. The mean body weights of the AOM-treated $APN^{-/-}$ C57BL/6J mice were not affected by administration of 50, 100 ppm SK-216, Pai-1 blocker. In APN-deficient C57BL/6J mice with 0, 50, 100 ppm SK-216 treatment, the mean numbers of ACFs/colon were 27.7, 23.1, and 18.4 ($P < .05$), respectively (Supplementary Table 3). Thus, Pai-1 blocker decreased colon ACF development in $APN^{-/-}$ C57BL/6J mice with AOM treatment.

Effects of APN Deficiency on Signal Transduction Events in Primary Cultured Cells

To study what happens to cell function in the absence of APN, fibroblasts were prepared from newborn $APN^{+/+}$ and $APN^{-/-}$ C57BL/6J mouse epidermis and treated with cell growth stimuli, insulin, or IL-6. Insulin treatment increased p-Akt and -Erk1/2 levels in both fibroblasts (Figure 2*E*). Interestingly, p-Akt and -Erk1/2 levels were increased 3.3- and 3.8-fold, respectively, by the treatment with IL-6 for 10 minutes in APN-knockout fibroblasts. Moreover, Bcl-2 was clearly expressed in APN-knockout fibroblasts compared with APN-wild fibroblasts.

Discussion

This study provided evidence that APN plays a pivotal role in intestinal carcinogenesis in mice. Thus, APN-deficient *Min* mice showed a 2- or 3-fold increase in the total number of intestinal polyps compared to those of APN-wild *Min* mice in both males and females at the ages of 9 and 12 weeks. In addition, APN-deficient *Min* mice exhibited increased serum Pai-1 levels with the *APN*-gene dosage. In addition, APN-deficient C57BL/6J mice treated with AOM demonstrated increased incidences and multiplicities of colorectal tumors, again with gene dosage-dependence, and serum Pai-1 levels tended to be increased with APN-deficiency at the age of 55 weeks.

In the $APN^{+/-}$ *Min* mice, serum APN levels were almost half those of $APN^{+/+}$*Min* mice, consistent with the gene dosage. Serum APN was not detected in $APN^{-/-}$*Min* mice. Numbers of intestinal polyps in *Min* mice were also associated with *APN*-gene dosage (Table 1 and Supplementary Table 1). Moreover, the effects of APN deficiency could be reversed by administration of APN (Supplemen-

tary Table 2). Other factors that might affect intestinal polyp development were not largely changed. For instance, expression levels of APN receptors, Adipo-R1 and -R2, and AdipoR-binding proteins, RACK1 and CK2β, were not affected by the genotype. Body weights and serum lipid levels also did not significantly vary. Of note, serum TG levels increased age dependently and also with a tendency for increase with the *APN*-gene dosage (Supplementary Figure 1). These data indicated that the amount of APN strongly affects development of intestinal polyps. In 12-week-old *APN*$^{-/-}$*Min* mice, the number of intestinal polyps was slightly decreased compared to those of *APN*$^{+/-}$*Min* mice. Several factors, such as an achievement of maximum levels of polyp development, serum TG levels, or some general dysfunctions, may influence polyp numbers, but further examinations are needed to clarify mechanisms.

It has been reported that 22-week short-term administration of a high-fat diet, but not normal diet, enhanced ACFs and tumor development in the colon of APN-deficient C57BL/6J mice.[21] The discrepancy in results between our study and this previous report could be due to the differences in the experimental period and diet. We followed the previous chemical-induced carcinogenesis protocol[22,23] and our findings added evidence that APN itself can suppress development of colon cancer under normal diet condition. It is assumed that abolished signaling from Adipo-R1 could enhance cell growth. It is known that activation of AMPK is decreased with APN deficiency in the colon epithelial cells. AMPKα activation through Adipo-R1 inhibits Akt followed by mammalian target of rapamycin inactivation.[21,24] The phosphatidylinositol 3 kinase/Akt signal pathway has been reported to activate signals for cell survival, cell growth, and the cell cycle leading to carcinogenesis.[25] We confirmed that abolished signaling from Adipo-R1 reduces AMPK activation (Figure 2*A*, *B*, and *C*), and increases Akt activation (Figure 2*D*). Therefore, we suggest that the AMPK/mammalian target of rapamycin/Akt pathway is possibly involved in the protective effect of APN against colon carcinogenesis. Moreover, primary cell cultures of fibroblasts from *APN*$^{+/+}$ or *APN*$^{-/-}$ C57BL/6J mice indicated that cells lacking APN are relatively responsive to growth stimuli and resistant to apoptosis through expressing Bcl-2,[26] which may support the growth advantage of neoplastic cells in APN-deficient mice.

APN acts as a regulator of adipocytokines. Under starvation conditions, APN activates AMPK in the hypothalamus to promote food intake and inhibits leptin activation.[27] In peripheral tissues, such as skeletal muscle, APN activates AMPK, IRS-1, and FATP-1, to stimulate fatty-acid combustion and glucose intake, which are inhibited by TNFα activation. It is assumed that APN deficiency affects other adipocytokine production in vivo, and can also affect intestinal tumorigenesis. Indeed, in the present study, serum levels of Pai-1 were significantly increased in the *APN*$^{+/-}$ and *APN*$^{-/-}$ C57BL/6J and *Min* mice. Treatment with an AMPK activator also reduced hepatic Pai-1 mRNA levels in *Min* mice, in line with earlier reports.[28,29] Thus, it is conceivable that Pai-1 expression levels are usually depressed by APN through Adipo-R1 receptor activity. We have recently demonstrated that Pai-1 blockers suppress intestinal polyp development in *Min* mice.[11] Thus, increased expression of Pai-1 could affect intestinal polyp development in *APN*$^{+/-}$*Min* and *APN*$^{-/-}$*Min* mice. Moreover, Pai-1 blocker was shown to decrease AOM-induced colon ACF formation in *APN*$^{-/-}$ C57BL/6J mice, indicating that increased expression of Pai-1 could affect colon carcinogenesis in *APN*$^{+/-}$ and *APN*$^{-/-}$ C57BL/6J mice.

In conclusion, this study indicated that hypoadiponectinemia promotes intestinal polyp development in *Min* mice, and also colon tumor development in AOM-treated C57BL/6J mice. AMPK inactivation belonging with Pai-1 induction and Akt activation was suggested to be the underlying mechanism for lack of APN on tumor growth. Further development of reagents that could elevate concentrations of APN is of interest. APN receptor agonists could be candidates for chemopreventive agents against colorectal cancer. Furthermore, as it is becoming more evident that a metabolic syndrome status promotes carcinogenesis in rodents and human, our results provide clues to a better understanding of mechanisms underlying colorectal carcinogenesis.

Supplementary Material

Note: To access the supplementary material accompanying this article, visit the online version of *Gastroenterology* at www.gastrojournal.org, and at doi: 10.1053/j.gastro.2011.02.019.

References

1. Trevisan M, Liu J, Muti P, et al. Markers of insulin resistance and colorectal cancer mortality. Cancer Epidemiol Biomarkers Prev 2001;10:937–941.
2. Colangelo LA, Gapstur SM, Gann PH, et al. Colorectal cancer mortality and factors related to the insulin resistance syndrome. Cancer Epidemiol Biomarkers Prev 2002;11:385–391.
3. Ahmed RL, Schmitz KH, Anderson KE, et al. The metabolic syndrome and risk of incident colorectal cancer. Cancer 2006;107:28–36.
4. Stocks T, Lukanova A, Johansson M, et al. Components of the metabolic syndrome and colorectal cancer risk; a prospective study. Int J Obes (Lond) 2008;32:304–314.
5. Giovannucci E. Insulin and colon cancer. Cancer Causes Control 1995;6:164–179.
6. Matsuzawa Y. The metabolic syndrome and adipocytokines. FEBS Lett 2006;580:2917–2921.
7. Otake S, Takeda H, Suzuki Y, et al. Association of visceral fat accumulation and plasma adiponectin with colorectal adenoma: evidence for participation of insulin resistance. Clin Cancer Res 2005;11:3642–3646.
8. Yamauchi T, Kamon J, Ito T, et al. Cloning of adiponectin receptors that mediate antidiabetic metabolic effects. Nature 2003;423:762–769.

9. Niho N, Takahashi M, Shoji Y, et al. Dose-dependent suppression of hyperlipidemia and intestinal polyp formation in Min mice by pioglitazone, a PPAR gamma ligand. Cancer Sci 2003;94:960–964.
10. Niho N, Takahashi M, Kitamura T, et al. Concomitant suppression of hyperlipidemia and intestinal polyp formation in APC-deficient mice by peroxisome proliferators-activated receptor ligands. Cancer Res 2003;63:6090–6095.
11. Mutoh M, Niho N, Komiya M, et al. Plasminogen activator inhibitor-1 (Pai-1) blockers suppress intestinal polyp formation in Min mice. Carcinogenesis 2008;29:824–829.
12. Kubota N, Terauchi Y, Yamauchi T, et al. Disruption of adiponectin causes insulin resistance and neointimal formation. J Biol Chem 2002;277:25863–25866.
13. Berg AH, Combs TP, Du X, Brownlee M, Scherer PE. The adipocyte-secreted protein Acrp30 enhances hepatic insulin action. Nat Med 2001;7:947–953.
14. Yamauchi T, Kamon J, Waki H, et al. The fat-derived hormone adiponectin reverses insulin resistance associated with both lipoatrophy and obesity. Nat Med 2001;7:941–946.
15. Otani K, Kitayama J, Yasuda K, et al. Adiponectin suppresses tumorigenesis in $Apc^{Min/+}$ mice. Cancer Lett 2010;288:177–182.
16. Sutherland LA, Bird RP. The effect of chenodeoxycholic acid on the development of aberrant crypt foci in the rat colon. Cancer Lett 1994;76:101–107.
17. Tsuchida A, Yamauchi T, Ito Y, et al. Insulin/Foxo1 pathway regulates expression levels of adiponectin receptors and adiponectin sensitivity. J Biol Chem 2004;279:30817–30822.
18. Ploplis VA, Balsara R, Sandoval-Cooper MJ, et al. Enhanced in vitro proliferation of aortic endothelial cells from plasminogen activator inhibitor-1-deficient mice. J Biol Chem 2004;279:6143–6151.
19. Li X, Shi X, Liang DY, Clark JD. Spinal CK2 regulates nociceptive signaling in models of inflammatory pain. Pain 2005;115:182–190.
20. Yuspa SH, Harris CC. Altered differentiation of mouse epidermal cells treated with retinyl acetate *in vitro*. Exp Cell Res 1974;86:95–105.
21. Fujisawa T, Endo H, Tomimoto A, et al. Adiponectin suppresses colorectal carcinogenesis under the high-fat diet condition. Gut 2008;57:1531–1538.
22. Shoji Y, Takahashi M, Kitamura T, et al. Downregulation of prostaglandin E receptor subtype EP3 during colon cancer development. Gut 2004;53:1151–1158.
23. Kawamori T, Kitamura T, Watanabe K, et al. Prostaglandin E receptor subtype EP1 deficiency inhibits colon cancer development. Carcinogenesis 2005;26:353–357.
24. Luo Z, Saha AK, Xiang X, et al. AMPK, the metabolic syndrome and cancer. Trends Pharmacol Sci 2005;26:69–76.
25. Huang XF, Chen JZ. Obesity, the PI3K/Akt signal pathway and colon cancer. Obes Rev 2009;10:610–616.
26. Konturek PC, Burnat G, Rau AT, Hahn EG, Konturek S. Effect of adiponectin and ghrelin on apoptosis of Barrett adenocarcinoma cell line. Dig Dis Sci 2008;53:597–605.
27. Kubota N, Yano W, Kubota T, et al. Adiponectin stimulates AMP-activated protein kinase in the hypothalamus and increases food intake. Cell Metab 2007;6:55–68.
28. Anfosso F, Chomiki N, Alessi MC, et al. Plasminogen activator inhibitor-1 synthesis in human hepatoma cell line Hep G2. Metformin inhibits the stimulating effect of insulin. J Clin Invest 1993;91:2185–2193.
29. He G, Pedersen SB, Bruun JM, et al. Metformin, but not thiazolidinediones, inhibits plasminogen activator inhibitor-1 production in human adipose tissue in vitro. Horm Metab Res 2003;35:18–23.

Received January 14, 2010. Accepted February 14, 2011.

Reprint requests

Address requests for reprints to: Michihiro Mutoh, MD, PhD, Cancer Prevention Basic Research Project, National Cancer Center Research Institute, 5-1-1 Tsukiji, Chuo-ku, Tokyo 104-0045, Japan. e-mail: mimutoh@ncc.go.jp; fax: +81-3-3543-9305.

Conflicts of interest

The authors disclose no conflicts.

Funding

This work was supported by Grants-in-Aid for Cancer Research, for the Third-Term Comprehensive 10-Year Strategy for Cancer Control from the Ministry of Health, Labour, and Welfare of Japan, and by the grant provided by The Ichiro Kanehara Foundation.

Supplementary Table 1. Number of Intestinal Polyps in Female Adiponectin-Deficient *Min* Mice

		No. of polyps/mouse				
		Small intestine				
Ages (wk)	APN genotype	Proximal	Middle	Distal	Colon	Total
9	+/+	2.6 ± 1.2	12.8 ± 4.7	36.4 ± 14.6	0.2 ± 0.2	52.0 ± 20.5
	+/−	4.0 ± 0.8	32.5 ± 7.0	128.7 ± 18.1[a]	0.5 ± 0.2	165.7 ± 25.6[a]
	−/−	5.6 ± 0.6[b]	37.1 ± 2.6[a]	132.3 ± 4.8[a]	1.0 ± 0.3	176.0 ± 5.6[a]
12	+/+	4.3 ± 1.2	19.4 ± 4.3	53.0 ± 12.8	0.1 ± 0.1	76.9 ± 17.7
	+/−	6.9 ± 1.6	46.0 ± 8.5[b]	123.0 ± 13.0[a]	1.0 ± 0.4	176.9 ± 22.0[a]
	−/−	6.4 ± 1.1	35.3 ± 1.6[a]	115.0 ± 9.8[a]	1.4 ± 0.4	158.1 ± 9.7[a]

NOTE. Data are mean ± standard error.
APN, adiponectin.
[a]$P < .01$ vs *APN*$^{+/+}$*Min*.
[b]$P < .05$ vs *APN*$^{+/+}$*Min*.

Supplementary Table 2. Number of Intestinal Polyps in 12-Week-Old *APN*$^{+/-}$*Min* Mice Treated With or Without Adiponectin

		No. of polyps/mouse				
		Small intestine				
Sex	APN (IP)	Proximal	Middle	Distal	Colon	Total
Male	–	5.4 ± 0.9	35.0 ± 4.9	103.6 ± 14.1	1.2 ± 0.4	145.2 ± 18.4
		3.3 ± 0.6	9.3 ± 1.5[a]	26.1 ± 6.2[a]	0.8 ± 0.3	39.5 ± 7.9[a]
Female	–	4.0 ± 0.8	25.2 ± 3.2	70.7 ± 11.5	0.6 ± 0.3	100.5 ± 14.9
		3.4 ± 0.9	12.5 ± 3.1[b]	27.9 ± 8.2[a]	0.2 ± 0.1	44.0 ± 12.0[a]

NOTE. Data are mean ± standard error (n = 10).
APN, adiponectin; IP, intraperitoneal.
[a]$P < .01$ vs corresponding sex without APN treatment.
[b]$P < .05$ vs corresponding sex without APN treatment.

Supplementary Table 3. Number of Azoxymethane-Induced Colonic Aberrant Crypt Foci in *APN*−/−C57BL/6J Mice Treated With SK-216

		No. of aberrant crypt foci/colon				
SK-216 (ppm)	No. of animals	Proximal	Middle	Distal	Rectum	Total
0	8	0.4 ± 0.2	3.6 ± 1.0	12.6 ± 1.6	11.0 ± 2.3	27.7 ± 3.4
50	9	0.7 ± 0.3	1.9 ± 0.6	12.7 ± 1.5	7.9 ± 0.7	23.1 ± 2.1
100	8	0.0	1.6 ± 0.7	9.6 ± 1.0	7.1 ± 1.7	18.4 ± 1.9[a]

NOTE. Data are mean ± standard error.
[a]$P < .05$ vs 0 ppm.

Enhancement of Carcinogenesis and Fatty Infiltration in the Pancreas in *N*-Nitrosobis(2-Oxopropyl)Amine-Treated Hamsters by High-Fat Diet

Mika Hori, PhD, Tsukasa Kitahashi, PhD,† Toshio Imai, PhD,‡ Rikako Ishigamori, PhD,* Shinji Takasu, PhD,* Michihiro Mutoh, MD, PhD,* Takashi Sugimura, MD, PhD,* Keiji Wakabayashi, PhD,*§ and Mami Takahashi, PhD**

Objectives: Obesity is associated with increased pancreatic cancer risk, although the mechanisms have yet to be detailed. This study aimed to elucidate promotion of pancreatic cancer by obesity and hyperlipidemia.

Methods: Six-week-old female Syrian golden hamsters were treated with *N*-nitrosobis(2-oxopropyl)amine (BOP) and after 1 week were fed a high-fat diet (HFD) or standard diet (STD) for 6 or 17 weeks.

Results: Body weight and serum levels of lipids and leptin were significantly higher in the HFD than the STD group at 14 weeks of age. Pancreatic ductal adenocarcinomas developed only in the BOP + HFD group, with an incidence of 67% ($P < 0.01$) at 14 weeks of age. In addition, the multiplicity was 2-fold greater in the BOP + HFD group than in the BOP + STD group ($P < 0.05$) at 25 weeks of age. Pancreatic fatty infiltration was increased by BOP treatment and further enhanced by the HFD, correlating with progression of BOP-induced pancreatic ductal adenocarcinoma and up-regulated expression of adipocytokines and cell proliferation–related genes in the pancreas.

Conclusions: High-fat diet is shown to increase serum lipid levels and enhance fatty infiltration in the pancreas with abnormal adipocytokine production, which may accelerate and enhance pancreatic cancer.

Key Words: pancreatic cancer, hamster, fatty infiltration, hyperlipidemia, adipocytokine

(*Pancreas* 2011;40: 1234–1240)

Pancreatic cancer is one of the most lethal human cancers, with a 5-year survival rate generally less than 5%.[1] High incidences of pancreatic cancer are reported in developed countries, and the frequency increased from the 1950s to 1990s in Japan.[2] Epidemiological studies have shown that environmental factors such as cigarette smoking, dietary habits, and diseases such as chronic pancreatitis and diabetes are associated with pancreatic cancer risk.[2] Recent evidence suggests that obesity is also associated with an increased risk of pancreatic cancer.[3,4] Furthermore, elevated serum triglycerides (TGs) and a high intake of cholesterol may exert potential promotion on pancreatic carcinogenesis.[5,6] However, the promoting mechanisms of these factors on pancreatic carcinogenesis have yet to be completely elucidated.

As in the United States and in Europe, the prevalence of metabolic syndrome is growing rapidly in Japan and Southeast Asia. Because this may result in an increase in pancreatic cancer, it is important to elucidate the mechanisms for the purpose of cancer prevention. The Syrian golden hamster is in a hyperlipidemic state even under normal diet conditions because lipoprotein lipase activity in the liver is low compared with mice and rats.[7] The hamster is a unique model animal for the development of pancreatic ductal adenocarcinomas (PDACs) induced by the subcutaneous injections of *N*-nitrosobis(2-oxopropyl)amine (BOP).[8] Histopathologically, the induced lesions possess close similarities to pancreatic cancer in humans. Moreover, point mutations in codon 12 of the *K-ras* gene are frequently observed, and expression of the *fragile histidine triad gene* is aberrant in BOP-treated hamsters,[9,10] as is also observed in human PDACs.[11,12] The *p16* gene is one of the most frequently inactivated tumor suppressor genes in human PDACs,[13] and loss of *p16* expression has also been found in hamster PDAC lesions.[14]

We previously demonstrated that pioglitazone, a peroxisome proliferator–activated receptor γ ligand, improved hyperlipidemia and suppressed BOP-induced PDAC development.[7] In the present study, we examined whether aggravated hyperlipidemia with a high-fat diet (HFD) affects pancreatic carcinogenesis in BOP-treated hamsters and analyzed the possible involvement of serum lipids and adipocytokines.

MATERIALS AND METHODS

Animals and Chemicals

Five-week-old female Syrian golden hamsters were obtained from Japan SLC (Shizuoka, Japan) and acclimated to laboratory conditions for a week. They were housed 2 or 3 per plastic cage, with sterilized softwood chips as bedding, in an air-conditioned animal room, on a 12-hour light-dark cycle. As a standard diet (STD), CE-2 (crude fat, 4.8%; crude protein, 25.1%; total calories, 3.43 kcal/g [CLEA Japan, Tokyo, Japan]) was used, and 1 group of hamsters was fed Quick Fat diet (crude fat, 13.6%; crude protein, 24.2%; total calories, 4.06 kcal/g [CLEA Japan]) as the HFD. CE-2 contains soybean oils, and Quick Fat contains beef tallow as the main fats. Body weight and food consumption were measured weekly. Food and water

From the *Cancer Prevention Basic Research Project, †Cancer Prevention Basic Research Project, Central Animal Laboratory, ‡Central Animal Laboratory, National Cancer Center Research Institute, Tokyo; and §Graduate School of Nutritional and Environmental Sciences, University of Shizuoka, Shizuoka, Japan.

Received for publication October 21, 2010; accepted April 21, 2011.

Reprints: Mami Takahashi, PhD, Cancer Prevention Basic Research Project, National Cancer Center Research Institute, 1-1 Tsukiji 5-chome, Chuo-ku, Tokyo 104-0045, Japan (e-mail: mtakahas@ncc.go.jp).

This work was supported in part by Grants-in-Aid for Cancer Research (21-2-1); a grant of the Research Grant of the Princess Takamatsu Cancer Research Fund (08-24009); and a grant of the Third-Term Comprehensive 10-Year Strategy for Cancer Control, the US-Japan Cooperative Medical Science Program from the Ministry of Health, Labour and Welfare of Japan. M. Hori and S. Takasu are and T. Kitahashi was awardees of Research Resident Fellowships from the Foundation for Promotion of Cancer Research (Japan) for the Third-Term Comprehensive 10-Year Strategy for Cancer Control during the performance of the present research.

The authors declare no conflict of interest.

were available *ad libitum*. *N*-Nitrosobis(2-oxopropyl)amine was obtained from Nacalai Tesque (Kyoto, Japan).

Study of the Effects of an HFD on BOP-Induced Pancreatic Carcinogenesis in Hamsters

At 6 weeks of age, 87 of 117 hamsters were injected subcutaneously with BOP 4 times (on days 1, 3, 5, and 7) at a dose of 10 mg/kg body weight, whereas the remaining 30 received saline as vehicle controls. From 1 week after the last BOP treatment, 34 of 87 BOP-treated and 15 of 30 saline-treated hamsters were given the HFD. At 14 weeks of age, 11, 12, 9, and 9 hamsters in the BOP + STD, BOP + HFD, saline + STD, and saline + HFD groups, respectively, were killed under deep anesthesia. The splenic lobes of the pancreas of 3 hamsters in each group at 14 weeks of age were rapidly immersed in RNA Later (Ambion, Austin, Tex) for RNA protection and stored at −80°C until RNA extraction. At 25 weeks of age, the remaining animals were killed. Finally, 11, 12, 9, and 9 hamsters at 14 weeks of age and 42, 22, 6, and 6 hamsters at 25 weeks of age, respectively, were in BOP + STD, BOP + HFD, saline + STD, and saline + HFD groups, respectively. Blood samples were collected in all cases from the abdominal aorta. Visceral fat weights were assessed by weighing total adipose tissues surrounding uteri after dissection. At autopsy, the pancreas, heart, lungs, kidneys, liver, and bile duct were carefully examined macroscopically and then fixed in 10% phosphate-buffered formalin (pH 7.4). Each pancreas was carefully dissected from surrounding tissue and fixed after spreading on filter paper except for frozen pancreas for RNA extraction at 14 weeks of age. All paraffin-embedded organs were sectioned and stained with hematoxylin and eosin for assessment of histopathological features. Pancreatic lesions were histopathologically diagnosed as dysplasia and adenocarcinomas. Dysplasia corresponds to lesions in human that are called PanIN 3.The experimental protocol was in accordance with the guidelines for Animal Experiments in the National Cancer Center and was approved by the Institutional Ethics Review Committee for Animal Experimentation.

Levels of Blood Glucose, Serum Lipids, Adipocytokines, and Insulin

Blood glucose levels were measured using an automatic blood glucose meter (Medisafe-mini GR-102; Terumo, Tokyo, Japan). The levels of TGs and total cholesterol (TC) in the serum were analyzed using the FUJI Dri-Chem system (Fuji Film, Tokyo, Japan). Serum free fatty acid (FFA) levels were assayed by an enzymatic method (SRL, Tokyo, Japan). Serum leptin (B-Bridge International, Inc, Mountain View, Calif), adiponectin (R&D Systems, Inc, Minneapolis, Minn), and insulin (Millipore Corp, Billerica, Mass) were examined using enzyme-linked immunosorbent assay kits according to the manufacturer's instructions.

Quantification of Pancreatic Adipocytes

The percentage areas of adipocytes infiltrated in the splenic lobe relative to total areas of splenic lobe on each pancreatic section were calculated using Win ROOF image analysis software (Mitani Corp, Tokyo, Japan). Pancreatic splenic lobes without adenocarcinomas were chosen because pancreatitis associated with invasive growth of adenocarcinomas may damage parenchyma cells and cause further fatty infiltration.

Reverse Transcription–Polymerase Chain Reaction Analysis

Total RNA was extracted from the pancreatic tissue using an RNeasy lipid tissue mini kit (Qiagen, GmbH, Hilden, Germany) combined with RNase-free DNase I (Invitrogen, Carlsbad, Calif), for degradation of genomic DNA. After RNA purification, aliquots of total RNA were subjected to reverse transcription (RT) reaction with oligo-dT and 9-mer random primers using an iScript cDNA Synthesis Kit (Bio-Rad Laboratories, Hercules, Calif). Each mRNA transcript was measured by a quantitative polymerase chain reaction (PCR) method with the DNA Engine Opticon 2 System (MJ Research, Waltham, Mass) and SYBR-Green chemistry (Bio-Rad Laboratories, Hercules, Calif) using the primer sets shown in Table 1. Data were calculated as ratios to 40S ribosomal protein S7 (RPS7) mRNA.

Statistical Analysis

The significance of differences in the incidences of dysplasia and PDAC was analyzed by the χ^2 test. Variation in other data was evaluated by the Student t test. $P < 0.05$ was regarded as significant.

RESULTS

Accelerated Body Weight Gain by the HFD

After the treatment of hamsters with a pancreatic carcinogen, BOP, at 6 weeks of age, the hamsters were fed an HFD or STD. The HFD group started to gain body weight at a greater rate than the STD group after 1-week feeding, and the difference

TABLE 1. The Primer Sequence Used for RT-PCR

Gene	Sequence
Leptin	
Forward primer (5′-3′)	CACCGGTTTGGACTTCATTC
Reverse primer (5′-3′)	CCACCACCTCTGTGGAGTAG
Plasminogen activator inhibitor 1	
Forward primer (5′-3′)	GTGCCCATGATGGCTCAGA
Reverse primer (5′-3′)	CGGGGCAGCCTGGTCATGTT
FASN	
Forward primer (5′-3′)	CTCAAGAAGGTGATCCGGGA
Reverse primer (5′-3′)	ACAGGGCTCACCAGGTTGTT
Monocyte chemoattractant protein 1	
Forward primer (5′-3′)	CTACAGCTTCTTTGGGACAC
Reverse primer (5′-3′)	AATGCCCCACTCACCTGCTG
IL-1β	
Forward primer (5′-3′)	CTTCATCTTTGAAGAAGAGC
Reverse primer (5′-3′)	TGTACAAAGCTCATGGAGAA
COX-2	
Forward primer (5′-3′)	AATGAGTACCGCAAACGCTT
Reverse primer (5′-3′)	GAGAGACTGAATTGAGGCAG
Insulin	
Forward primer (5′-3′)	GACCATCAGCAAGCAGGTCA
Reverse primer (5′-3′)	ACTGATCCACAATGCCACGC
IGF-1	
Forward primer (5′-3′)	GAGCTGGTGGACGCTCTTCA
Reverse primer (5′-3′)	TCAGATCACAGCTCCGGAAG
Cyclin D1	
Forward primer (5′-3′)	CCATGGAACACCAGCTCCTG
Reverse primer (5′-3′)	CGGTCCAGGTAGTTCATGGC
RPS7	
Forward primer (5′-3′)	CCAGAAAATCCAAGTCCGGC
Reverse primer (5′-3′)	AGTCCTCAAGGATGGCATCG

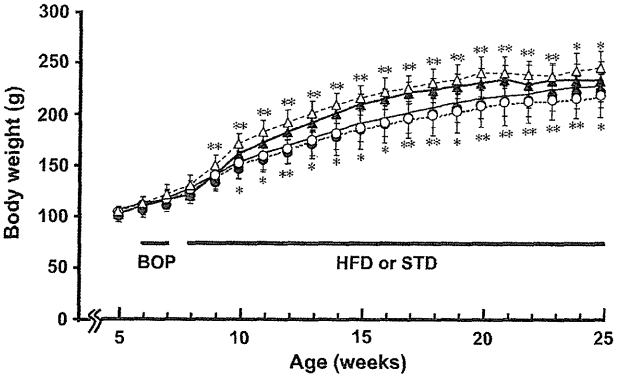

FIGURE 1. Body weight curves for the STD groups (circles) and the HFD groups (triangles) treated with BOP (closed symbols) or saline (open symbols). Data are means ± SD. Asterisks show the significance between the BOP + STD and BOP + HFD groups (upper) and between the saline + STD and saline + HFD groups (lower). $*P < 0.05$ and $**P < 0.01$ vs the respective STD group.

was obvious at 14 weeks of age (181 ± 9.6 vs 158 ± 13 g; $P < 0.01$; Fig. 1). Body weight curves reached plateaus at 25 weeks of age in the BOP + HFD and BOP + STD groups (214 ± 19 vs 203 ± 16 g; $P < 0.05$). Average values for food intake in the HFD and STD groups treated with BOP were almost the same, at 10.6 ± 0.3 g and 11.0 ± 0.8 g, respectively, whereas average calorie intake (kcal/hamster per day) was higher in the HFD group than in the STD group (43.1 ± 1.1 vs 37.9 ± 2.7; $P < 0.01$). Effects of BOP treatment on body weights and food intake were not observed.

Increases in the Levels of Serum Lipids With the HFD

At 14 weeks of age, the levels of serum lipids (TGs, TC, and FFAs) were significantly higher in the HFD than the STD groups, with and without BOP treatment (Table 2). Visceral fat weights in the HFD groups were significantly increased as compared with the STD groups. At 25 weeks of age, serum TG, TC, and FFA levels in the BOP + HFD group still remained higher than those in the BOP + STD group. However, increases of serum TC and FFA levels from 14 to 25 weeks of age were more apparent in the STD groups than in the HFD groups, resulting in smaller differences between the two. Interestingly, serum FFA levels were significantly higher in the BOP-treated than saline groups at 25 weeks of age.

Enhancement of Pancreatic Fatty Infiltration by the HFD

Fatty infiltration in hamster pancreatic tissues (Figs. 2A–D) was found to be characterized by infiltration of adipocytes into the intralobular spaces, without accumulation of fat within the parenchyma cells. Overall, adipocytes were diffusely present in the parenchyma tissues with particular accumulations around blood vessels. In the splenic lobes without PDACs, estimated percentage areas of adipocytes per area of pancreas were 4.4%, 7.4%, 7.9%, and 14.5% in the saline + STD, BOP + STD, saline + HFD, and BOP + HFD groups, respectively, at 14 weeks of age, with increase to 14.7%, 27.3%, 24.9%, and 41.9%, respectively, at 25 weeks of age (Fig. 2E). Fatty infiltration was increased by BOP treatment and also by the HFD feeding. In the BOP + HFD group, synergistic effects were observed.

Enhancement of PDAC Development and Increase of PDAC With Fatty Infiltration by the HFD

During the experiment, single animals in the BOP + STD and BOP + HFD groups died because of PDAC development at 19 and 21 weeks of age, respectively. The incidences and multiplicities of dysplasia as precancerous lesions and PDACs are summarized in Table 3. The incidence of dysplasia in the BOP + HFD group was higher than that in the BOP + STD group at 14 weeks of age and further increased at 25 weeks of age. Of note, PDACs developed only in the BOP + HFD group at 14 weeks of age at an incidence of 67%. The PDAC incidences at 25 weeks of age were similar at 80% and 86% in the BOP + STD and BOP + HFD groups, respectively, but the multiplicities of dysplasia and PDACs in the BOP + HFD group were 6- and 2-fold, respectively, of those in the

TABLE 2. Levels of Serum Lipids and Visceral Fat Weights in Hamsters

Group	Age, wks	No. Animals*	TGs, mg/dL	TC, mg/dL	FFAs, μEQ/L	Visceral Fat, g
BOP + STD	14	11	382 ± 87	188 ± 20	1058 ± 345	4.1 ± 2.2
BOP + HFD	14	12	510 ± 125†‡	269 ± 29†	1458 ± 320†	6.5 ± 1.8†
Saline + STD	14	9	402 ± 131	197 ± 38	1099 ± 319	3.3 ± 1.1
Saline + HFD	14	9	802 ± 196§	274 ± 90‖	1749 ± 338§	6.8 ± 2.3§
BOP + STD	25	10	344 ± 144	242 ± 23¶	1891 ± 306¶	10.1 ± 2.1¶
BOP + HFD	25	10	563 ± 126†	307 ± 64†	2214 ± 145†‡	11.3 ± 2.6¶
Saline + STD	25	4	284 ± 118	240 ± 30	1462 ± 292#	10.9 ± 2.2¶
Saline + HFD	25	3	546 ± 138§¶	317 ± 17§	1784 ± 234§	13.2 ± 2.0¶

Values are presented as mean ± SD.

*No. of animals assessed for visceral fat weight was 36 in the BOP + STD, 18 in the BOP + HFD, 6 in the saline + STD, and 6 in the saline + HFD groups at 25 weeks of age.

†$P < 0.01$ vs BOP + STD group.

‡$P < 0.01$ vs saline + HFD group.

§$P < 0.01$ vs saline + STD group.

‖$P < 0.05$ vs saline + STD group.

¶$P < 0.01$ vs the respective group at 14 weeks of age.

#$P < 0.05$ vs BOP + STD group.

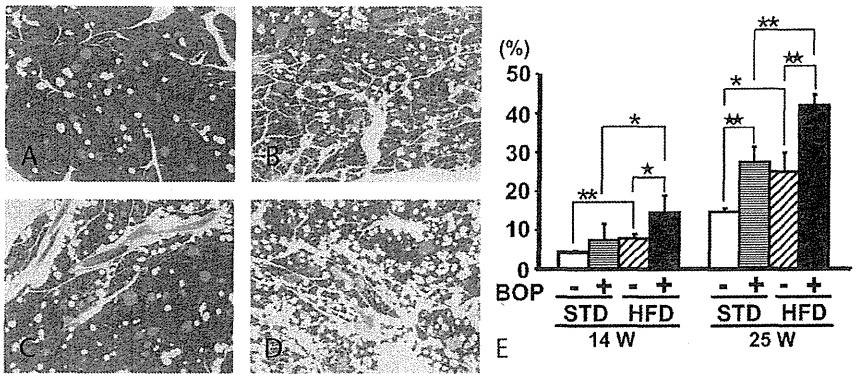

FIGURE 2. Effects of BOP treatment and the HFD feeding on fatty infiltration in the hamster pancreas. Representative data for hematoxylin-eosin–stained hamster pancreatic tissues in the saline + STD (A), BOP + STD (B), saline + HFD (C), and BOP + HFD (D) groups at 25 weeks of age are shown. Quantification of adipocyte areas per splenic lobe without PDAC was performed for each pancreas (n = 3–6, E). Open columns show the saline + STD group. Striped columns show the BOP + STD group. Hatched columns are for the saline + HFD group and closed columns for the BOP + HFD group. Original magnification ×40 for (A–D). *$P < 0.05$ and **$P < 0.01$ vs the respective value in the STD group. ★$P < 0.05$ and ★★$P < 0.01$ vs the respective value in the saline group.

TABLE 3. Incidences and Multiplicities of BOP-Induced Pancreatic Lesions

		No. Animals With Lesions, %		No. Lesions/Animal	
Group	**Age, wks**	**Dysplasia**	**Adenocarcinoma**	**Dysplasia**	**Adenocarcinoma**
BOP + STD	14	2/8 (25)	0/8 (0)	0.83 ± 0.98*	0
BOP + HFD	14	7/9 (78)†	6/9 (67)‡	1.00 ± 0.71	1.14 ± 0.69‡
BOP + STD	25	27/41 (66)	33/41 (80)	1.02 ± 0.91	1.66 ± 1.37
BOP + HFD	25	21/21 (100)‡	18/21 (86)	6.05 ± 2.84‡	3.19 ± 3.54†

*Mean ± SD.
†$P < 0.05$ vs BOP + STD group.
‡$P < 0.01$ vs BOP + STD group.

BOP + STD group. Figure 3 shows the sizes of PDACs at 25 weeks of age. In the BOP + HFD group, PDACs were rather larger than those in the BOP + STD group, especially the number of PDACs 2 to 3 mm in diameter being significantly higher.

Interestingly, adipocytes within PDACs were observed in large amounts in the BOP + HFD group at 25 weeks of age (Fig. 4A) but were a few in the BOP + STD group (Fig. 4B). Figure 4C shows the numbers of PDACs, classified according to the degree of fatty infiltration in BOP-treated hamsters. The HFD increased the number of PDAC with fatty infiltration within PDAC and its surrounding tissue. Differences between the BOP + HFD and BOP + STD groups were not observed in the numbers of PDAC without fatty infiltration.

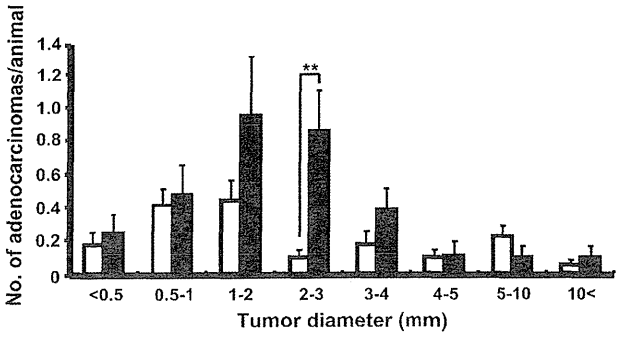

FIGURE 3. Size distributions of PDACs at 25 weeks of age. The numbers of each size of PDAC per hamster are given for the BOP + STD group (white bars) and BOP + HFD group (black bars). **$P < 0.01$ vs BOP + STD group.

In BOP-treated hamsters, it has been reported that carcinomas were induced in the bile duct, kidneys, liver, and lungs in addition to the pancreas.[8] At 14 weeks of age, no carcinomas were observed except for PDACs. At 25 weeks of age, cholangiocellular, hepatocellular, and lung carcinomas developed in the BOP + HFD group, and their incidences tended to be higher than in the BOP + STD group (cholangiocellular carcinomas: 71% vs 50%, hepatocellular carcinomas: 9.5% vs 7.1%, lung carcinomas: 33% vs 26%). No carcinomas were observed in the saline groups given either the HFD or the STD.

Increases in Serum Adipocytokine Levels and Pancreatic mRNA Expression Levels of Adipocytokine and Inflammatory- and Proliferation-Associated Genes by the HFD

As described above, differences of body weights and serum lipids between the BOP + HFD and the BOP + STD groups were obvious at 14 weeks of age, and PDACs were observed only in the BOP + HFD group at 14 weeks of age (Tables 2 and 3). Thus,

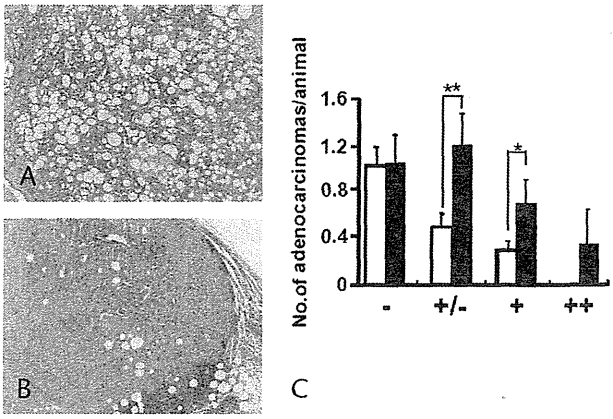

FIGURE 4. The levels of fatty infiltration within PDACs at 25 weeks of age. Representative data for fatty infiltration in PDACs in the BOP + HFD group (A) and BOP + STD group (B). The numbers of PDAC per hamster are given for the BOP + STD group (white bars) and BOP + HFD group (black bars) and are classified according to the degree of fatty infiltration per hamster (C). No fatty infiltration (−), fatty infiltration in surrounding tissue of PDAC (±), moderate fatty infiltration within PDAC (+; <10%), marked fatty infiltration within PDAC (++; ≥10%). Original magnification ×100 for (A and B). *$P < 0.05$ and **$P < 0.01$ vs BOP + STD group.

the serum levels of adipocytokines and insulin and mRNA expression levels of adipocytokines and inflammatory- and proliferation-associated genes in the pancreatic splenic lobes were compared between the BOP + STD and BOP + HFD groups at this time point. Serum leptin levels in the BOP + HFD group were 2 times higher than those in the BOP + STD group (21.7 ± 6.3 vs 10.4 ± 4.7 ng/mL; $P < 0.01$). In addition, serum adiponectin levels were higher in the BOP + HFD group than in the BOP + STD group (14.6 ± 2.0 vs 12.5 ± 1.5 ng/mL; $P < 0.05$). The levels of serum insulin (10.4 ± 3.1 vs 7.9 ± 3.0 ng/mL) and blood glucose (135 ± 25 vs 128 ± 31 mg/dL) did not significantly differ between the BOP + HFD and BOP + STD groups.

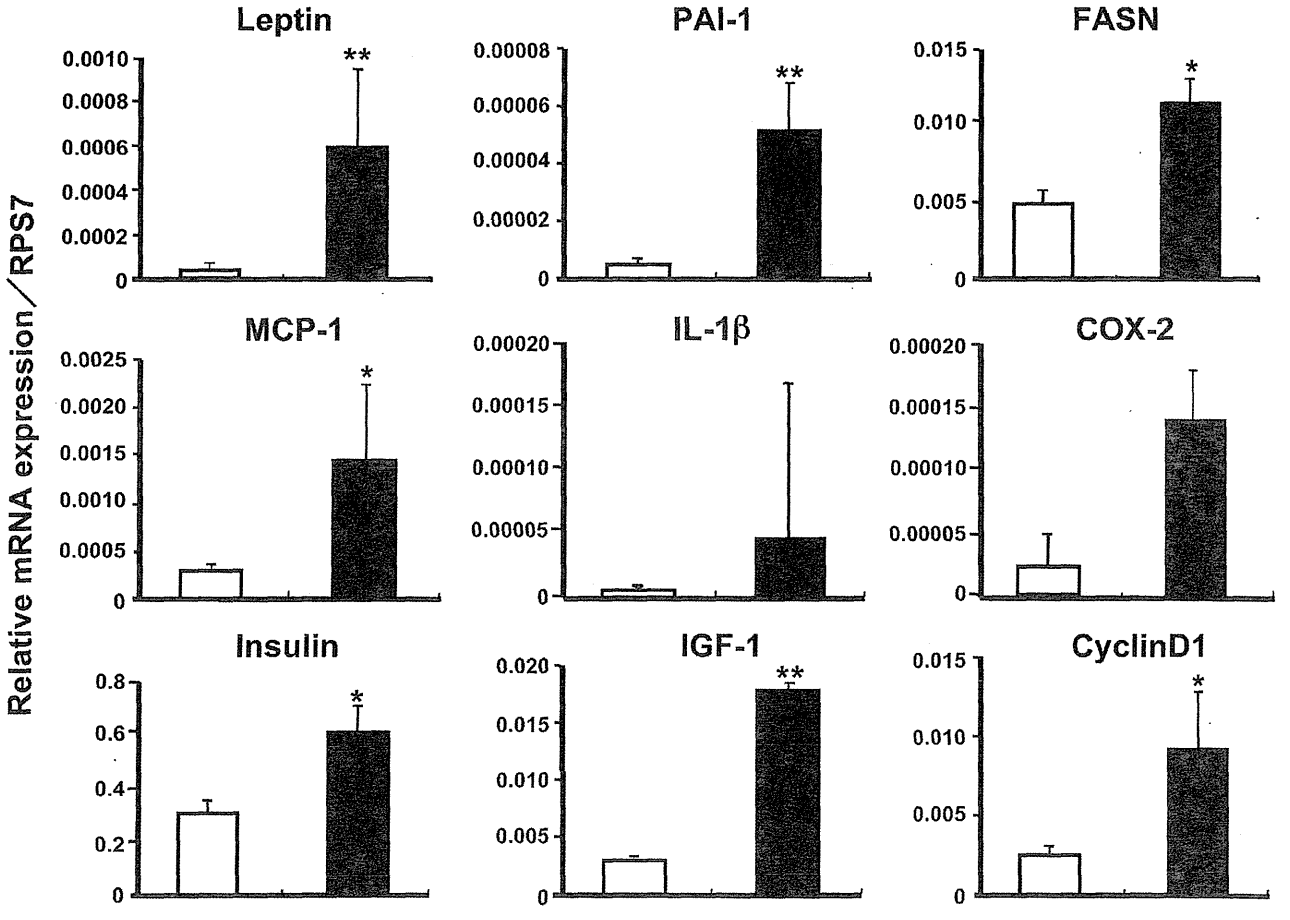

FIGURE 5. Expression levels of adipocytokines and inflammatory- and proliferation-associated genes in the hamster pancreas. Expression analysis of genes encoding adipocytokines and inflammatory- and proliferation-associated factors in the pancreatic tissue of BOP-treated hamsters fed either STD or HFD was conducted by real-time RT-PCR. The amounts of mRNA were normalized and shown relative to that of RPS7 mRNA in each sample with ranges determined by evaluating the expression: $2^{-\Delta\Delta CT}$ with $\Delta\Delta C_T$ + the SD of the $\Delta\Delta C_T$ value and $\Delta\Delta C_T$ − the SD of the $\Delta\Delta C_T$ value. Open columns, the BOP + STD group; closed columns, the BOP + HFD group. *$P < 0.05$ and **$P < 0.01$ vs the BOP + STD group.

mRNA levels in the pancreas for adipocytokines and lipid metabolism–related genes such as leptin, plasminogen activator inhibitor 1, and fatty acid synthase (FASN) were significantly higher in the BOP + HFD group than in the BOP + STD group (Fig. 5). Expression of inflammatory-related genes, including monocyte chemoattractant protein 1, IL-1β, and cyclooxygenase 2 (COX-2), also was increased or tended to be increased in the BOP + HFD group. The levels of mRNAs encoding growth-related genes such as insulin, insulin like growth factor I (IGF-I), and cyclin D1 were also elevated in the pancreas in the BOP + HFD group, indicating enhanced proliferation by the HFD.

DISCUSSION

In the present study, aggravated hyperlipidemia due to an HFD accelerated PDAC development with elevated serum levels of lipids and leptin. Moreover, pancreatic fatty infiltration and expression of adipocytokines and inflammation- and growth-associated genes in the pancreas were enhanced, indicating possible involvement in the mechanisms of promotion of PDAC development.

It has been reported that a high-corn-oil diet increased PDAC development in BOP-treated hamsters as compared with a low-corn-oil diet.[15] Furthermore, a diet containing beef tallow has been shown to increase PDAC development compared with a diet containing corn oil, although the amount of fat did not affect the yield of PDAC at 84 weeks of age.[16] Our present data using an HFD containing beef tallow as the main fat source showed early development of cancer at 14 weeks of age and higher yield of pancreatic dysplasia and PDAC at 25 weeks of age compared with the STD. Animal fats such as beef tallow are rich in cholesterol and saturated acids, and their intake has been shown to increase the levels of serum lipids.[17,18] Indeed, the HFD used in the present study made BOP-treated hamsters more hyperlipidemic compared with the STD. These findings suggest that the elevation of serum TG and TC levels was associated with PDAC development in addition to higher caloric intake by the HFD.

In the present study, serum FFAs was increased with HFD intake at 14 weeks of age and further enhanced in the BOP-treated groups at 25 weeks of age (Table 2). Moreover, the expression of FASN was observed to be enhanced in the pancreas tissues of the BOP + HFD-treated hamsters, indicating *de novo* FFA synthesis. In the case of Wistar rats, long-term intake of an HFD significantly increased body weight and serum lipids and then induced chronic pancreatic injury and microcirculatory disturbance.[19] Furthermore, in the present study, serum FFA levels correlated with pancreatic fatty infiltration in the BOP-treated groups (Table 2; Fig. 2). A high level of FFAs is reported to be toxic to various cells, probably because of peroxidation.[20,21] In addition to pancreatic injury induced by BOP, FFAs could damage pancreatic tissue and induce fatty infiltration.

The serum levels of leptin and adiponectin and visceral fat weights in the BOP + HFD group were higher than those in the BOP + STD group at 14 weeks of age (Table 2). Blood glucose levels did not significantly differ between the BOP + HFD and BOP + STD groups. Serum adiponectin is reported to correlate with insulin sensitivity.[22] Thus, it was indicated that insulin resistance was not caused in hamsters fed an HFD in the present study, although a hyperlipidemic state, hyperleptinemia, and accumulated visceral obesity were apparent. Leptin is reported to stimulate proliferation in colon,[23] breast[24] and prostate cancers,[25] and pancreatic β cells.[26] Furthermore, recent epidemiological studies have provided evidence that elevated circulating leptin levels are associated with obesity-related colon, breast, and prostate cancers.[27] Although the correlation between circulating leptin levels and cancer development remains inconclusive, in the present study, a correlation with hamster visceral fat and the incidence of PDAC was noted.

In addition, the expression levels of IL-1β and COX-2 also tended to increase in the BOP + HFD group (Fig. 5), and it has been shown that these are induced by leptin in rat brain and human endometrial cancer cells.[28,29] Overproduction of prostaglandin E_2 by COX-2 has been suggested to cause cell proliferation, angiogenesis, and antiapoptosis.[30,31] Other growth factors such as insulin and IGF-1 were also elevated in the pancreas of HFD-fed hamsters in the present study (Fig. 5). These growth factors have been reported to upregulate FASN.[32,33] Serum and tissue levels of IGF-1 may be increased in pancreatic cancer,[34] this factor being known to stimulate cell proliferation[35] with bidirectional crosstalk between leptin and IGF-1 signaling to promote cancer invasion.[36] Thus, the elevation of leptin, insulin, and IGF-1 in the hamster pancreas by the HFD in the present study could indicate promotion of cancer development through increases of inflammation- and growth-associated gene expression.

In humans, a high body mass index, elevated visceral fat weight and serum lipids, and diabetes mellitus have been shown to be the risk factors for pancreatic fatty infiltration.[37,38] Triglycerides and FFAs cause fatty infiltration in the pancreas in humans and animals, and obesity and diabetes mellitus are established risk factors for pancreatic cancer in humans.[3,4] Furthermore, pancreatic fatty infiltration has been clinically shown to promote dissemination of pancreatic cancer[39] and to increase the risk of pancreatic fistula after pancreaticoduodenectomy.[40] These available data suggest that it may alter the tumor microenvironment, enhance tumor spread, and be involved in progression of pancreatic cancer.

In conclusion, the present study demonstrated that an HFD accelerated PDAC development along with elevation of serum lipids and leptin. Moreover, enhanced pancreatic fatty infiltration and expression of adipocytokines in the pancreas were suggested to be involved in the promotion of PDAC development. Further clarification of mechanisms in detail and generation of evidence of involvement in humans are clearly warranted.

ACKNOWLEDGMENTS

The authors thank Ms Ruri Nakanishi and Mr Naoaki Uchiya for expert technical assistance.

REFERENCES

1. Maitra A, Hruban RH. Pancreatic cancer. *Annu Rev Pathol.* 2008;3:157–188.
2. Lowenfels AB, Maisonneuve P. Epidemiology and prevention of pancreatic cancer. *Jpn J Clin Oncol.* 2004;34:238–244.
3. Li D, Morris JS, Liu J, et al. Body mass index and risk, age of onset, and survival in patients with pancreatic cancer. *JAMA.* 2009;301:2553–2562.
4. Inoue M, Noda M, Kurahashi N, et al. Impact of metabolic factors on subsequent cancer risk: results from a large-scale population-based cohort study in Japan. *Eur J Cancer Prev.* 2009;18:240–247.
5. Tulinius H, Sigfússon N, Sigvaldason H, et al. Risk factors for malignant diseases: a cohort study on a population of 22,946 Icelanders. *Cancer Epidemiol Biomarkers Prev.* 1997;6:863–873.
6. Lin Y, Tamakoshi A, Hayakawa T, et al. Nutritional factors and risk of pancreatic cancer: a population-based case-control study based on direct interview in Japan. *J Gastroenterol.* 2005;40:297–301.
7. Takeuchi Y, Takahashi M, Sakano K, et al. Suppression of *N*-nitrosobis(2-oxopropyl)amine-induced pancreatic carcinogenesis in hamsters by pioglitazone, a ligand of peroxisome

proliferator-activated receptor gamma. *Carcinogenesis.* 2007;28:1692–1696.
8. Pour P, Althoff J, Krüger FW, et al. A potent pancreatic carcinogen in Syrian hamsters: *N*-nitrosobis(2-oxopropyl)amine. *J Natl Cancer Inst.* 1977;58:1449–1453.
9. Fujii H, Egami H, Chaney W, et al. Pancreatic ductal adenocarcinomas induced in Syrian hamsters by *N*-nitrosobis(2-oxopropyl)amine contain c-Ki-ras oncogene with a point-mutated codon 12. *Mol Carcinog.* 1990;3:296–301.
10. Tsujiuchi T, Sasaki Y, Kubozoe T, et al. Alterations in the *Fhit* gene in pancreatic duct adenocarcinomas induced by *N*-nitrosobis(2-oxopropyl)amine in hamsters. *Mol Carcinog.* 2003;36:60–66.
11. Grünewald K, Lyons J, Fröhlich A, et al. High frequency of Ki-ras codon 12 mutations in pancreatic adenocarcinomas. *Int J Cancer.* 1989;43:1037–1041.
12. Sorio C, Baron A, Orlandini S, et al. The *FHIT* gene is expressed in pancreatic ductular cells and is altered in pancreatic cancers. *Cancer Res.* 1999;59:1308–1314.
13. Caldas C, Hahn SA, da Costa LT, et al. Frequent somatic mutations and homozygous deletions of the p16 (MTS1) gene in pancreatic adenocarcinoma. *Nat Genet.* 1994;8:27–32.
14. Hanaoka M, Shimizu K, Shigemura M, et al. Cloning of the hamster p16 gene 5′ upstream region and its aberrant methylation patterns in pancreatic cancer. *Biochem Biophys Res Commun.* 2005;333:1249–1253.
15. Birt DF, Salmasi S, Pour PM. Enhancement of experimental pancreatic cancer in Syrian golden hamsters by dietary fat. *J Natl Cancer Inst.* 1981;67:1327–1332.
16. Birt DF, Julius AD, Dwork E, et al. Comparison of the effects of dietary beef tallow and corn oil on pancreatic carcinogenesis in the hamster model. *Carcinogenesis.* 1990;11:745–748.
17. Lawson N, Jennings RJ, Pollard AD, et al. Effects of chronic modification of dietary fat and carbohydrate in rats. *Biochem J.* 1981;200:265–273.
18. Pitt HA. Hepato-pancreato-biliary fat: the good, the bad and the ugly. *HPB.* 2007;9:92–97.
19. Yan MX, Li YQ, Meng M, et al. Long-term high-fat diet induces pancreatic injuries via pancreatic microcirculatory disturbance and oxidative stress in rats with hyperlipidemia. *Biochem Biophys Res Commun.* 2006;347:192–199.
20. Morita Y, Yoshikawa T, Takeda S, et al. Involvement of lipid peroxidation in free fatty acid–induced isolated rat pancreatic acinar cell injury. *Pancreas.* 1998;17:383–389.
21. Mylonas C, Kouretas D. Lipid peroxidation and tissue damage. *In Vivo.* 1999;13:295–309.
22. Yamauchi T, Kamon J, Waki H, et al. The fat-derived hormone adiponectin reverses insulin resistance associated with both lipoatrophy and obesity. *Nat Med.* 2001;7:941–946.
23. Hardwick JC, Van Den Brink GR, Offerhaus GJ, et al. Leptin is a growth factor for colonic epithelial cells. *Gastroenterology.* 2001;121:79–90.
24. Dieudonne MN, Machinal-Quelin F, Serazin-Leroy V, et al. Leptin mediates a proliferative response in human MCF7 breast cancer cells. *Biochem Biophys Res Commun.* 2002;293:622–628.
25. Somasundar P, Frankenberry KA, Skinner H, et al. Prostate cancer cell proliferation is influenced by leptin. *J Surg Res.* 2004;118:71–82.
26. Okuya S, Tanabe K, Tanizawa Y, et al. Leptin increases the viability of isolated rat pancreatic islets by suppressing apoptosis. *Endocrinology.* 2001;142:4827–4830.
27. Garofalo C, Surmacz E. Leptin and cancer. *J Cell Physiol.* 2006;207:12–22.
28. Inoue W, Poole S, Bristow AF, et al. Leptin induces cyclooxygenase-2 via an interaction with interleukin-1beta in the rat brain. *Eur J Neurosci.* 2006;24:2233–2245.
29. Gao J, Tian J, Lv Y, et al. Leptin induces functional activation of cyclooxygenase-2 through JAK2/STAT3, MAPK/ERK, and PI3K/AKT pathways in human endometrial cancer cells. *Cancer Sci.* 2009;100:389–395.
30. Kuwano T, Nakao S, Yamamoto H, et al. Cyclooxygenase 2 is a key enzyme for inflammatory cytokine-induced angiogenesis. *FASEB J.* 2004;18:300–310.
31. Iñiguez MA, Rodríguez A, Volpert OV, et al. Cyclooxygenase-2: a therapeutic target in angiogenesis. *Trends Mol Med.* 2003;9:73–78.
32. Paulauskis JD, Sul HS. Hormonal regulation of mouse fatty acid synthase gene transcription in liver. *J Biol Chem.* 1989;264:574–577.
33. Zeng L, Biernacka KM, Holly JMP, et al. Hyperglycaemia confers resistance to chemotherapy on breast cancer cells: the role of fatty acid synthase. *Endocr Relat Cancer.* 2010;17:539–551.
34. Karna E, Surazynski A, Orłowski K, et al. Serum and tissue level of insulin-like growth factor-I (IGF-I) and IGF-I binding proteins as an index of pancreatitis and pancreatic cancer. *Int J Exp Pathol.* 2002;83:239–245.
35. Ma J, Sawai H, Matsuo Y, et al. IGF-1 mediates PTEN suppression and enhances cell invasion and proliferation via activation of the IGF-1/PI3K/Akt signaling pathway in pancreatic cancer cells. *J Surg Res.* 2010;160:90–101.
36. Saxena NK, Taliaferro-Smith L, Knight BB, et al. Bidirectional crosstalk between leptin and insulin-like growth factor-I signaling promotes invasion and migration of breast cancer cells via transactivation of epidermal growth factor receptor. *Cancer Res.* 2008;68:9712–9722.
37. Rosso E, Casnedi S, Pessaux P, et al. The role of "fatty pancreas" and of BMI in the occurrence of pancreatic fistula after pancreaticoduodenectomy. *J Gastrointest Surg.* 2009;13:1845–1851.
38. Lee JS, Kim SH, Jun DW, et al. Clinical implications of fatty pancreas: correlations between fatty pancreas and metabolic syndrome. *World J Gastroenterol.* 2009;15:1869–1875.
39. Mathur A, Zyromski NJ, Pitt HA, et al. Pancreatic steatosis promotes dissemination and lethality of pancreatic cancer. *J Am Coll Surg.* 2009;208:989–994.
40. Mathur A, Pitt HA, Marine M, et al. Fatty pancreas: a factor in postoperative pancreatic fistula. *Ann Surg.* 2007;246:1058–1064.

Hindawi Publishing Corporation
Biochemistry Research International
Volume 2012, Article ID 398697, 8 pages
doi:10.1155/2012/398697

Review Article

Lipoprotein Lipase as a Candidate Target for Cancer Prevention/Therapy

Shinji Takasu, Michihiro Mutoh, Mami Takahashi, and Hitoshi Nakagama

Division of Cancer Development System, National Cancer Center Research Institute, 5-1-1 Tsukiji, Chuo-ku, Tokyo 104-0045, Japan

Correspondence should be addressed to Michihiro Mutoh, mimutoh@ncc.go.jp

Received 28 April 2011; Accepted 17 August 2011

Academic Editor: Terry K. Smith

Epidemiological studies have shown that serum triglyceride (TG) levels are linked with risk of development of cancer, including colorectal and pancreatic cancers, and their precancerous lesions. Thus, it is assumed that serum TG plays an important role in carcinogenesis, and the key enzyme lipoprotein lipase (LPL), which catalyzes the hydrolysis of plasma TG, may therefore be involved. Dysregulation of LPL has been reported to contribute to many human diseases, such as atherosclerosis, chylomicronaemia, obesity, and type 2 diabetes. Recently, it has been reported that *LPL* gene deficiency, such as due to chromosome 8p22 loss, *LPL* gene polymorphism, and epigenetic changes in its promoter region gene, increases cancer risk, especially in the prostate. In animal experiments, high serum TG levels seem to promote sporadic/carcinogen-induced genesis of colorectal and pancreatic cancers. Interestingly, tumor suppressive effects of LPL inducers, such as PPAR ligands, NO-1886, and indomethacin, have been demonstrated in animal models. Moreover, recent evidence that LPL plays important roles in inflammation and obesity implies that it is an appropriate general target for chemopreventive and chemotherapeutic agents.

1. Introduction

A high-calorie diet and low physical activity, part of the so-called "Westernization" of lifestyle, are associated with elevated incidences of the breast, colon, liver, pancreas, and prostate cancers. Moreover, they are also linked with the risk of obesity, type 2 diabetes, and dyslipidemia. The World Cancer Research Fund and American Institute for Cancer Research have evaluated causal relationships between body fat and cancer and provided strong evidence for roles in such as colorectum and pancreas cancers [1]. In Japan, overweight and obesity (body mass index ≥25) are reported to be associated with cancers of specific organs, such as the colorectum (male), postmenopausal breast (female), and the liver in individuals positive for hepatitis C virus infection [2–4].

Greater body fatness is a major risk factor for the metabolic syndrome, which presents as a combination of symptoms, such as dyslipidemia (elevated triglyceride (TG) levels or low high-density lipoprotein (HDL) cholesterol), elevated blood pressure, and elevated fasting glucose levels. Hypertriglyceridemia is associated with the risk of colon cancer in Japanese men (HR = 1.71) and being overweight with the risk of breast cancer (HR = 1.75) [5]. In addition, most epidemiological studies, including our own, have consistently showed that serum TG levels are associated with the risk of colorectal adenoma, a precursor lesion of colorectal cancer [6–11]. Thus, it is assumed that serum TG could play an important role in carcinogenesis and that the key enzyme lipoprotein lipase (LPL), which catalyzes the hydrolysis of plasma TG, may also be involved. In this paper, we focus on the roles of LPL in cancer development and further discussed possible approaches to cancer prevention/therapy.

2. Function, Structure, and Gene Regulation of LPL

2.1. Functions and Structure of LPL. LPL plays an important role in lipid metabolism as an enzyme responsible for hydrolysis of the TG component in circulating chylomicrons and very-low-density lipoprotein (VLDL) via binding with apolipoprotein C2 [12, 13]. Thus, lowering or deficiency of LPL expression is associated with hyperlipidemia [14, 15]. The LPL enzyme itself is composed of two structurally

distinct regions. The amino-terminal domain is responsible for catalysis with a catalytic center formed by three amino acids (Ser^{132}, Asp^{156}, and His^{241}). The carboxy-terminal domain of LPL is required for its binding to the lipoprotein substrate [3, 16–18].

2.2. LPL Gene Expression and Its Regulation. The human *LPL* gene is located on chromosome 8p22 and composed of 10 exons [19]. LPL is ubiquitously expressed in the whole body, but especially in the adipose tissue and the skeletal muscle [20, 21] and is regulated by hormonal and inflammatory stimuli, such as insulin [22, 23], glucocorticoid [24, 25], adrenaline [26], tumor necrosis factor (TNF)-α [27, 28], transforming growth factor (TGF)-β [29], and interleukin (IL)-1β [27].

The expression of LPL is controlled transcriptionally and posttranscriptionally. Basal promoter activity has been shown to be regulated by Oct-1 and the NF-Y binding motifs [30, 31], and the 5′-CCTCCCCC-3′ motif, which interacts with Sp1 and Sp3 [32]. Induction of *LPL* gene transcription is mediated by the peroxisome proliferator response element (PPRE) and the responsible element which binds to sterol regulatory element-binding protein (SREBP) [33, 34]. The effect of insulin on *LPL* expression is an example of posttranscriptional control, the hormone being suggested to increase *LPL* mRNA levels via mRNA stabilization [23, 35].

3. Relationship between LPL and Cancer: Human Studies

3.1. Loss of LPL and Resultant Common Disease. LPL has been reported to play key roles in many human diseases, such as atherosclerosis, obesity, type 2 diabetes, chylomicronaemia, Alzheimer's disease, and cachexia [15]. Especially, *LPL* gene deficiency is the cause of type I hyperlipoproteinemia (familial hyperchylomicronemia) [36]. Homozygous deficiency of *LPL* in humans is rare, but heterozygous deficiency is observed in around 3% of people with various ethnic backgrounds [37, 38]. Although these individuals have elevated serum levels of TG and decreased HDL cholesterol [39], it is not clear whether they are at increased risk of atherosclerosis, ischemic heart disease, type 2 diabetes, and cancer. There is a report that the *LPL* S447X mutation is associated with a higher risk of pancreatic calcification and steatorrhea in hyperlipidemic pancreatitis [40]. Since LPL provides fatty acids to the tissues and fatty acids evoke insulin resistance, *LPL* gene deficiency could affect glucose metabolism. However, whether heterozygous *LPL* deficiency reduces plasma glucose levels or not is still controversial. One paper described reduction of plasma glucose levels, but two others observed no effects as compared with LPL intact humans [41–43]. On the other hand, it has been reported that patients with poorly controlled diabetes frequently have dyslipidemia due to defects in LPL enzyme activity [44].

3.2. Effects of Chromosome 8p22 Loss and LPL Gene Polymorphisms on Cancer Risk. Alteration in genomic DNA, such as point mutations and deletions/amplifications or epigenetic changes such as CpG island hypermethylation and histone modification, can induce abnormal gene expression, which in the case of tumor suppressor genes or oncogenes could eventually lead to carcinogenesis. The human *LPL* gene has been mapped to chromosome 8p22 and previous studies on loss of heterozygosity (LOH) in colorectal tumors suggested that a putative tumor suppressor gene may lie within the short arm of chromosome 8, that is, 8p22-p21.3. Loss of 8p23.1-22 is also reported to be an important stage in initiation or promotion of hepatocellular carcinoma development and may also be the most frequent chromosomal alteration in prostate cancer [45]. It has been found that deletion of *LPL* is observed in 68% (52/76) of localized prostate cancers by FISH analysis [46]. It has further been reported that chromosomal region 8p23.1-8p21.1 may harbor one or more important prostate-cancer-susceptible loci based on linkage analyses in 159 hereditary prostate cancer families [47, 48]. To date, several new candidate cancer-susceptible genes have been cloned to 8p22, such as *deleted in breast cancer 2* (*DBC2*), *leucine zipper tumor suppressor 1* (*LZTS1*), *deleted in liver cancer 1* (*DLC1*), and *mitochondrial tumor suppressor 1* (*MTUS1*) [49–52]. Thus, cancer-susceptible genes mapped close to the *LPL* gene could be affected by *LPL* gene deletion, and exert combined effects in promoting carcinogenesis.

Moreover, an *LPL* Ser447stop polymorphism has been shown to be associated with prostate cancer risk [53] and the *LPL* gene is commonly methylated in prostate tumors [54]. *LPL* promoter CpG island methylation has been revealed in 45% of LPL-deleted tumors and in 22% of LPL-retaining tumors [54]. Biallelic inactivation of *LPL* by chromosomal deletion and promoter methylation may thus contribute to prostate tumorigenesis, but information is lacking regarding pancreatic cancer.

4. Relationship between LPL and Cancer: Animal Studies

4.1. Dyslipidemia Observed in Cancer-High-Susceptibility Animal Models. Elevated serum TG has been shown to promote carcinogen-induced colon carcinogenesis, and rats with hypertriglyceridemia such as the Zucker obese and Nagase analbuminemic strains and F344 rats fed a high-fat diet are all known to be more sensitive to carcinogen treatments than rats with normal serum lipid levels [55–57].

In the case of mice, the Apc^{1309} (C57BL/6J$^{Apc/Apc\Delta 1309}$) [58] and Min (C57BL/6-$Apc^{Min/+}$) animal models of human familial adenomatous polyposis (FAP) feature development of large numbers of intestinal polyps and hypertriglyceridemia [59, 60]. Although no significant differences between Apc^{1309} mice and wild-type mice were observed at 6 weeks of age, the average serum TG value in the former at 12 weeks was obviously increased almost 10-fold (~600 mg/dL) over that at 6 weeks. Similar increase of TG levels (~400 mg/dL) was observed in Min mice at 15 weeks compared to 8 weeks of age (Table 1). Along with TG elevation, mRNA levels of *LPL* in the liver and small intestine of Apc^{1309} and Min mice were suppressed. Of note, other lipogenic genes, such as *FAS* and *stearoyl-CoA*